Chapter 2

Dislocation and disclination charges in a lattice

The description of structural defects, or topological singularities, which can appear within a solid, such as dislocations and disclinations, is a field of physics, initiated mainly by the idea of macroscopic defects of Volterra[1] in 1907, which has experienced very fast development during its very rich century of history, as Hirth[2] illustrated very well in 1985.

In this chapter, in order to describe the plasticity of solid lattices, we introduce an innovative concept of *density of dislocation and disclination charges* in Eulerian lattices, then we present a review of the macroscopic and microscopic topological singularities of the lattice which can be associated with dislocation and disclination charges. We then discuss the movement of dislocation charges within the lattice, by introducing the notion of dislocation charge flow, and we deduce the force acting on a dislocation charge, called *the Peach and Koehler force*. Finally, we present the potentialities inherent in this original approach of topological singularities within solid lattices in Euler coordinates.

Macroscopic concept of plastic distortion charges

In the previous chapter, we introduced the elastic and anelastic behaviors of a solid. There is yet another behavior that we will deal with now. If you take an aluminum bar and bend it slightly, it returns to its initial state if you release the stress that was applied to it, and this is elastic behavior. On the other hand, if it is folded very strongly and the stress is released, it no longer returns to its original state, but remains definitively folded. We speak in this case of *plastic behavior* and *plasticity* of the aluminum bar.

The description of the plasticity of a solid lattice is sometimes undertaken phenomenologically using a plastic distortion tensor $\vec{\beta}_i^{\,pl}$. However, this approach is extremely limited, in particular by the fact that there is no unequivocal relationship between the local state of plastic deformation and the microscopic state of the network of structural defects responsible for this plastic deformation. This is the reason why the way of expressing the presence of plastic distortions in a lattice must be approached so that it is possible to take into account the microscopic state of the network of structural defects. A very elegant way of carrying out this modification is to introduce the concepts of *densities and fluxes of dislocation charges*, responsible for *the plastic distortions* of the solid, as well as *densities of disclination charges*, responsible for *the plastic contortions* of the solid.

The concept of *charges of plastic distortions of the solid*, which will henceforth be called simply *dislocation charges* by language shortcuts, is intuitively simple to grasp, if one uses the approach[1] developed in 1907 by the Italian physicist Vito Volterra. The latter had the idea of

---

[1] *V. Volterra, «L'équilibre des corps élastiques», Ann. Ec. Norm. (3), XXIV, Paris, 1907*

[2] *J.-P. Hirth, «A Brief History of Dislocation Theory», Metallurgical Transactions A, vol. 16A, p. 2085, 1985*

considering a pipe of solid material and imagining, either that it is cut and that it is subjected to a certain distortion before being glued, or that one removes part of it before being glued again, as shown by the examples in figure 2.1. In these two examples, the deformations undergone by the solid after gluing are irreversible and irrecoverable, therefore of *plastic nature*.

On the other hand, it is intuitively clear that internal forces have developed inside the solid after gluing. These appeared during the elastic deformation which was imposed on the rest of the solid to make the two jaws to be bonded coincide. In fact, everything happens exactly as if a localized topological discontinuity had appeared in the center of the pipe after gluing, discontinuity which would be the source of *an elastic distortion field* in the macroscopically continuous medium which composes the pipe. And this distortion field, by its presence, is itself a source of a field of conjugate stresses, which can be called *internal stress field*.



Vito Volterra (1860-1940)

Mathematically, the discontinuity due to gluing should be able to be translated in terms of a local density of *"plastic charges"*, source of an elastic distortion field, and therefore of an internal stress field, in a completely similar way that in electromagnetism where the presence of a local density ρ of electric charges is responsible for the appearance of an electric displacement field $\vec{D}$, as shown by Maxwell's equation $\rho = \mathrm{div}\,\vec{D}$, and consequently of a conjugated electric field $\vec{E}$, since $\vec{D} = \varepsilon_0 \vec{E}$. The aim of this chapter will therefore be to show how it is possible to mathematically translate the phenomena of plasticity inside a solid, not only by introducing densities of plastic charges, but also flows of plastic charges, by analogy with the flow of electric charges $\vec{j}$ appearing in the equation $\vec{j} = -\partial\vec{D}/\partial t + \overrightarrow{\mathrm{rot}}\,\vec{H}$ of Maxwell's electromagnetism, in which $\vec{H}$ represents the magnetic field.

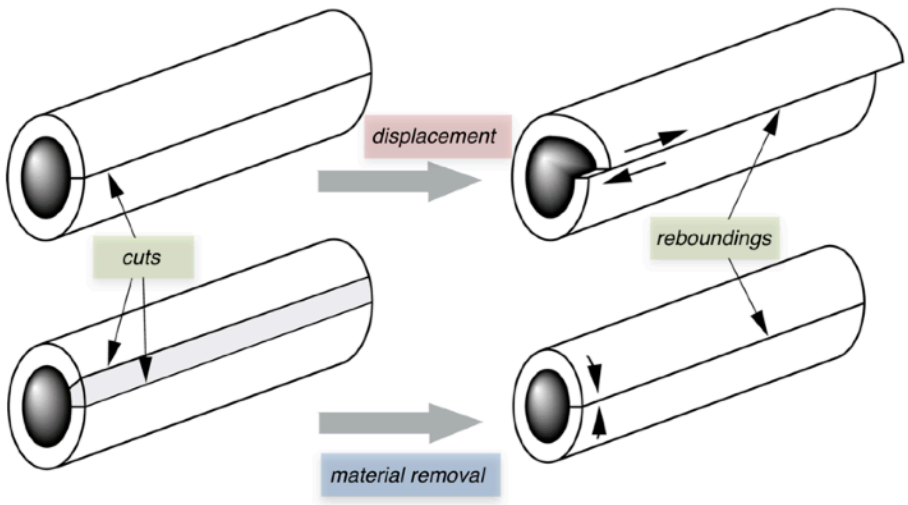

Figure 2.1 - *The famous "Volterra pipes"*

In figure 1.2, one saw that the condition of compatibility $\overrightarrow{\text{rot}}\,\vec{\beta}_i = 0$ prohibits the singularity by dislocation of the field of displacement $\vec{u}_E$. Consequently, *if the compatibility condition was no longer zero*, therefore if $\overrightarrow{\text{rot}}\,\vec{\beta}_i = \vec{\lambda}_i \neq \vec{0}$, the course on the closed contour $\boldsymbol{C}$ will result in the existence of a quantity $\vec{\boldsymbol{B}}$, which is called *macroscopic Burgers vector*, defined on the contour $\boldsymbol{C}$ and which corresponds to the macroscopic translation necessary to accommodate the medium to the presence of *density charges* $\vec{\lambda}_i$, in order to ensure compatibility of total deformations and rotations (the absence of voids and overlaps of matter within the solid).

The discontinuity $\vec{\boldsymbol{B}}$ is called a *macroscopic dislocation* of the solid, in the sense of Volterra, and one will consequently call *density of dislocation charges* the tensorial density of charges $\vec{\lambda}_i$ responsible for plastic distortions.

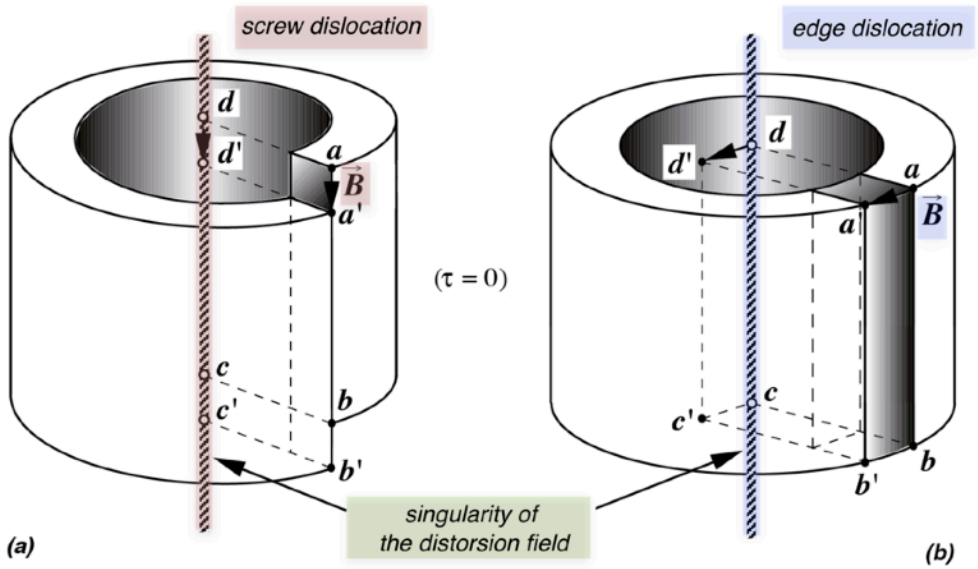

Figure 2.2 - *Realization de screw* ***(a)*** *and edge* ***(b)*** *dislocations by cutting and gluing*

Such macroscopic dislocation is carried out in a continuous solid by locally cutting this solid and by moving the two jaws of the cut parallel to each other, before gluing them again. This process is illustrated schematically in figure 2.2a using a pipe of material which is cut along the plane $\boldsymbol{abcd}$ and which is glued after parallel sliding of the interfaces in the direction of the cut. There then appears *a one-dimensional topological singularity* of the distortion field located on the axis $\boldsymbol{cd}$. This macroscopic singularity, characterized by a translation vector $\vec{\boldsymbol{B}}$ parallel to the line of singularity, is called *screw dislocation*.

On the other hand, if the two jaws are glued together by parallel translation of the jaws, perpendicular to the plane of the cut, and with the addition or subtraction of a parallelepiped of material (figure 8.2b), there appears another one-dimensional topological singularity of the distortion field, located on the axis $\boldsymbol{cd}$. This macroscopic singularity, characterized by a translation vector $\vec{\boldsymbol{B}}$ perpendicular to the line of singularity, is called *edge dislocation*. Another way of proceeding to achieve an edge-type dislocation, but without adding or subtracting material, is to glue the two jaws together after parallel translation of the jaws in the plane of the cut, perpendicular to the direction of the cut, as shown in figure 2.3. Under the *sine qua non* condition that

the elastic volume expansion of the medium remained zero during the plastic deformation process, the Burgers vector $\vec{B}$, obtained by the course on a contour C surrounding the singularity, corresponds exactly to the macroscopic translation which has undergone the jaw $abcd$.

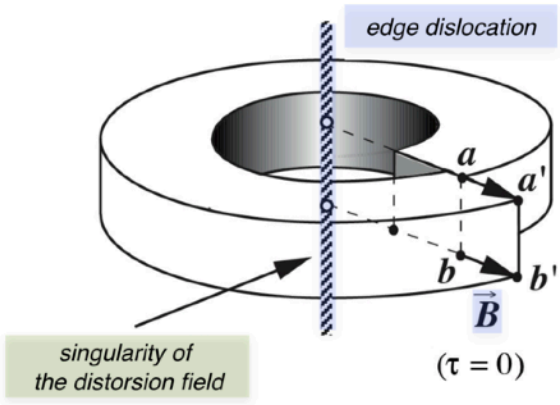

Figure 2.3 - *Other realization of an edge dislocation by cutting and gluing*

Under the condition that the elastic volume expansion τ of the medium remained zero during the plastic deformation process, the Burgers vector $\vec{B}$, obtained by the course on the contour C surrounding the singularity, then corresponds exactly to the macroscopic translation which the jaw $a'b'cd$ underwent. As the vector $\vec{B}$ must remain constant if we vary the diameter of the integration contour C or if we move this contour vertically, we deduce that *the dislocation charges must be confined to the immediate vicinity of the axis of the pipe*, and that *their tensor density must be a constant along this axis*.

One can also imagine that within a continuous solid one cuts a vacuum within the material in the shape of a torus, as illustrated by the section represented in figure 2.4a, then that one cuts the median plane located in the center torus. The two jaws ab and $a'b'$ thus formed can then be moved relative to each other, then glued.

The first possible case is to move the two jaws parallel to the cutting plane by a distance $\vec{B}$ as shown in figure 2.4b. After gluing, the medium is deformed by shearing and the torus contains a *macroscopic dislocation of slip loop type*, composed of edge, screw and mixed dislocation portions.

You can also insert additional material in the form of a thin disc with a thickness $\vec{B}$ between the two jaws and weld this disc to the two jaws (figure 2.4c). We then obtain a deformation of the medium responsible obviously for a curvature of the medium on both sides of the torus. The torus is then the site of *a macroscopic dislocation, of the prismatic loop type*. In this case, the prismatic loop is said to be *interstitial*, because it contains additional material, and it is composed of a single edge dislocation which closes on itself. A very similar case is obtained if, instead of adding a disc of material, we subtract a thin disc of material with a thickness $\vec{B}$, as illustrated in figure 2.4d. We also obtain *a macroscopic dislocation, of the prismatic loop type*, but this loop is said to be *lacunar*, because it lacks a certain amount of matter. Within the torus, there is also a single edge dislocation which closes on itself.

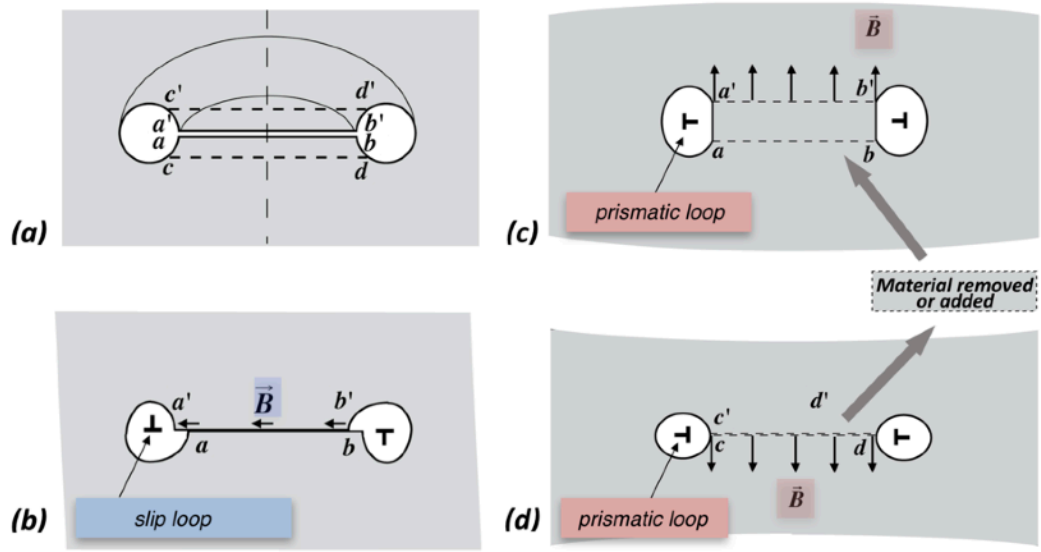

Figure 2.4 - *Initial cutting of a torus and its median plane to form loops* ***(a)*** *and making a slip dislocation loop by sliding the jaws* ***(b)*** *and prismatic dislocation loops by addition* ***(c)*** *or subtraction* ***(d)*** *of material.*

All the singularities thus obtained are obviously responsible for a field of distortion within the solid. Consequently, they require a non-zero formation energy. They are stabilized within the solid by re-bonding the two jaws of the cut, therefore by the bonds within the solid.

Definition of density and flow tensors of plastic charges

In figure 1.12, we represented the geometro-kinetic equations of the medium, which in fact connect the temporal variations of the distortions of the solid, calculated along the trajectory of the medium particles using the *material derivative*, with the spatial variations of the velocity field $\vec{\phi}(\vec{r},t)$ of the medium particles, calculated using the gradient of the components of the velocity field in the case of the distortion tensor. And in figures 1.13 to 1.15, we had introduced the geometro-compatibility equations, which ensured the continuity of the Eulerian field of displacement within the solid, therefore the absence of discontinuities of displacements like dislocations. In the presence of displacement discontinuities, like those which we have just described on the macroscopic scale, it becomes necessary to redefine the geometro-kinetic equations and the geometro-compatibility equations of the medium, in order to take into account the presence of these topological singularities of distortion.

Using the definition of the distortion tensor, as it was obtained in the previous chapter in the presence of plastic deformation, the total distortions $\vec{\beta}_i^{\,tot}$ are the sum of elastic, anelastic and plastic distortions, such as $\vec{\beta}_i^{\,tot} = \vec{\beta}_i^{\,él} + \vec{\beta}_i^{\,an} + \vec{\beta}_i^{\,pl}$. Another notation for these distortions can be introduced, which makes it possible to separate the contributions of plastic deformation from the contributions of elastic and anelastic deformation, by simply writing that $\vec{\beta}_i^{\,tot} \rightarrow \vec{\beta}_i + \vec{\beta}_i^{\,pl}$ with $\vec{\beta}_i = \vec{\beta}_i^{\,él} + \vec{\beta}_i^{\,an}$, as illustrated in figure 2.5 (a).

This simple change of name makes it possible to introduce, by analogy with the equations of

electromagnetism, the concept of *tensor density* $\vec{\lambda}_i$ *of charges*, responsible for plastic distortions, by assuming *a priori* the relation $\vec{\lambda}_i = -\overrightarrow{\text{rot}}\,\vec{\beta}_i^{\,pl}$ of definition of $\vec{\lambda}_i$ from the plastic distortion tensor $\vec{\beta}_i^{\,pl}$, as well as the concept of *tensor flow* $\vec{J}_i$ *of charges*, responsible for the temporal variation of plastic distortions, by supposing *a priori* the relation $\vec{J}_i = d\vec{\beta}_i^{\,pl} / dt$ of definition of $\vec{J}_i$, starting from the temporal derivative $d\vec{\beta}_i^{\,pl} / dt$ of the tensor of plastic distortion $\vec{\beta}_i^{\,pl}$. It should also be noted here that the concept of charge flow is defined as *a flow with respect to the lattice*, because it is deduced from the material derivative of $\vec{\beta}_i^{\,pl}$, that is to say from the temporal derivative of $\vec{\beta}_i^{\,pl}$ *taking along the trajectory of the solid lattice*.

The geometro-kinetic equation for the distortion tensor $\vec{\beta}_i$ in figure 1.12 already contained a source S_n of lattice sites, which actually represented a source of plasticity related to the volume expansion of the lattice. The geometro-kinetic equation for the distortion tensor $\vec{\beta}_i$ obtained in figure 2.5 (a) generalizes this fact, by including the source of lattice sites in the concept of *tensor flow* $\vec{J}_i$ *of plastic charges*.

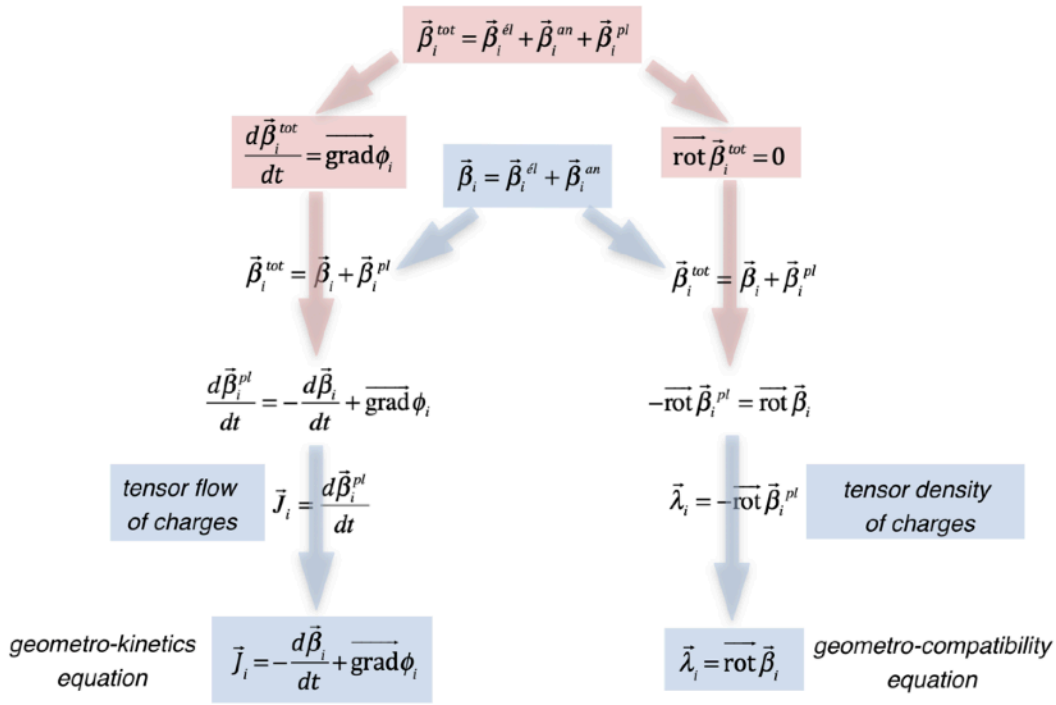

Figure 2.5(a) - *Introduction of the tensor of density and flux of plastic charges in the presence of elasticity, elasticity and plasticity*

The introduction of these new tensors of density and flow of charges is not free, because these answer at best the requirement to find a way to express the presence of plastic distortions in a solid so that it is possible to take into account the microscopic state of the network of structural defects in the solid. It will also be verified *a posteriori*, during the interpretation of these tensors in the rest of this chapter, that this way of proceeding is indeed judicious. With this approach to the phenomena of plasticity by tensors $\vec{J}_i$ and $\vec{\lambda}_i$, the topological equations describing the geometro-kinetics and the geometro-compatibility of the distortion tensor

$\vec{\beta}_i = \vec{\beta}_i^{\,él} + \vec{\beta}_i^{\,an}$ of an elastic, anelastic and plastic solid are now written in a much more general way, as illustrated in figure 2.5(a).

This new version of topological distortion tensors and geometro-kinetic equations is in fact nothing more than a simple change of terminology for plastic distortions, based on an analogy with the two Maxwell equations of electromagnetism $\rho = \mathrm{div}\,\vec{D}$ and $\vec{j} = -\partial\vec{D}/\partial t + \overrightarrow{\mathrm{rot}}\,\vec{H}$. Finding all the potentialities contained in this formulation of topological equations will therefore be the subject of the rest of this chapter.

The *density* $\vec{\lambda}_i$ *of dislocation charges* and the *flow* $\vec{J}_i$ *of dislocation charges* are tensor quantities, on which it is possible to apply symmetry operations to reduce their tensor order, i.e. to make them vector quantities and scalar quantities. These symmetry operations are shown in figure 2.5 (b).

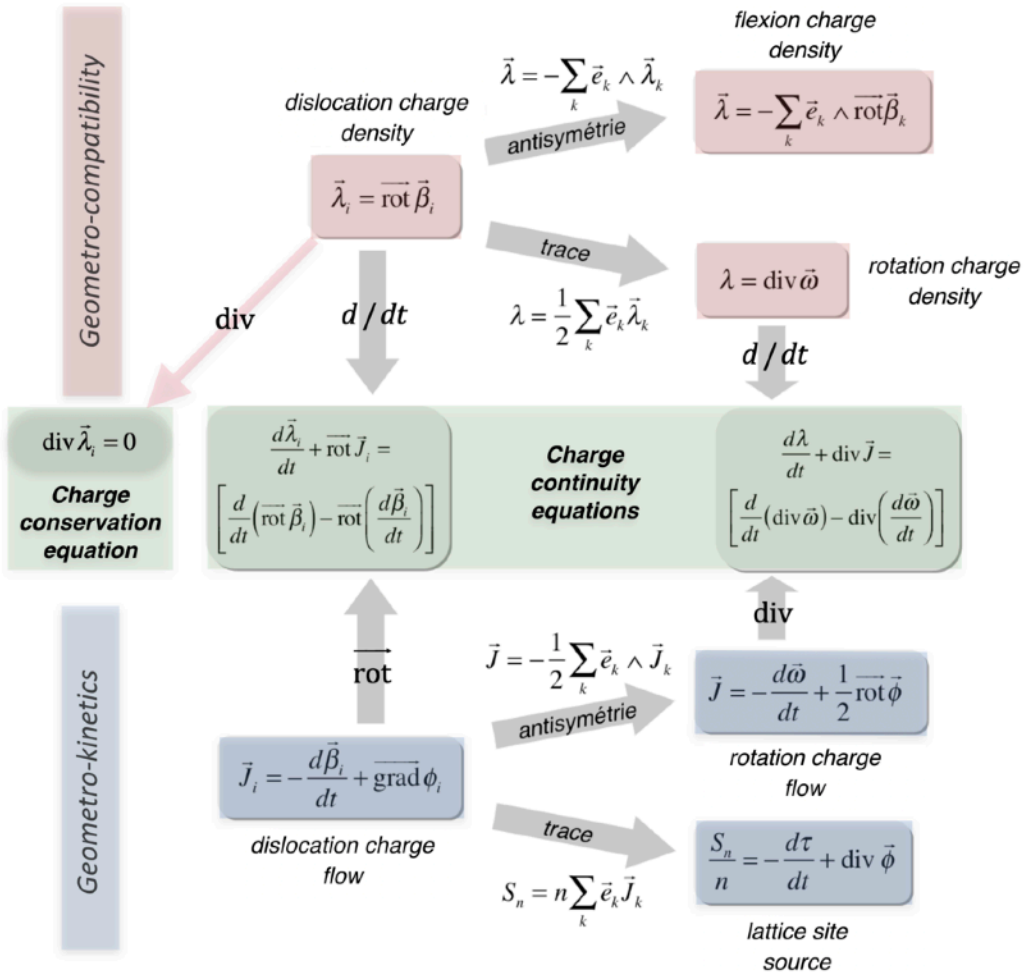

Figure 2.5(b) - *Breakdowns of charge densities and charge flows, and charge continuity and charge conservation equations*

Concerning the geometro-compatibility equations, we note that the tensorial density $\vec{\lambda}_i$ of dislocation charges contains *a vector density* $\vec{\lambda}$ *of bending charges* and *a scalar density* λ *of rotation charges*. We will return later to the interpretation of vector bending charges, but we can already give an interpretation of the effects of scalar rotation charges. Indeed, if we consider

figure 1.15, we know that the compatibility condition $\mathrm{div}\,\vec{\omega} = 0$ prohibits the singularity by divergence of the rotation field, which means that, if $\mathrm{div}\,\vec{\omega} = \lambda \neq 0$ within the volume ***V***, there can appear a field of rotation vectors which diverge, of the same way that the local presence of a non-zero density of electric charges at a place in space induces a diverging electric field.

Concerning the geometro-kinetic equations, we note that the tensor flow $\vec{J}_i$ of dislocation charges contains a *vectorial flow* $\vec{J}$ *of rotation charges* and that it re-appears the *scalar volume source* S_n *of lattice sites*.

The mathematical combination of the material derivative of the geometro-compatibility equations with the rotational or the divergence of the geometro-kinetic equations makes it possible to deduce *the continuity equations* of figure 2.5(b) for the plastic distortion charges, which link the temporal evolution of the densities of charge along the trajectory of the medium to the spatial variations of the charge flows. These continuity equations reveal rather surprising terms of sources of plastic charges, in the sense that these terms are associated with *the possible existence of a non-commutativity of the temporal operator of material derivative with the space operators*. Finally, as regards the tensorial density $\vec{\lambda}_i$ of dislocation charges, we note that it is linked to the curl of $\vec{\beta}_i$, so that it obligatorily satisfies the relation $\mathrm{div}\,\vec{\lambda}_i = 0$ of the vector analysis which we will call *the conservation equation of the dislocation charges*, equation which will be called thereafter to play a considerable role in the topological interpretation of the charges of dislocation.

Macroscopic concept of plastic contortion charges

In Figure 1.16, we reported the complete system of distortions and contortions of a solid lattice in Euler coordinates, in the case of a geometro-compatible solid. The same diagram, if it is drawn in the case of a solid with a non-zero density of dislocation charges $\vec{\lambda}_i$, becomes clearly more complex as illustrated in figure 2.6.

Apart from the tensor density $\vec{\lambda}_i$ of dislocation charges, the vector density $\vec{\lambda}$ of bending charges and the scalar density λ of rotation charges, which we will call 1st order charges associated with plastic distortions, there appear to be 2nd order charges, associated with plastic contortions, which will be called *the tensor density* $\vec{\theta}_i$ *of disclination charges* and *the scalar density* θ *of curvature charges*.

We also note that the expressions of *contortions* $\vec{\chi}_i$ *, flexions* $\vec{\chi}$ *and torsions* $\left[\vec{\chi}_i\right]^S$ of the solid lattice become much more complicated since they now call in their respective expressions for the existence of *charge densities of contortion, of flexion and of torsion of 1st order*, deduced as combinations of the charge densities of dislocation $\vec{\lambda}_i$, of flexion $\vec{\lambda}$ and of rotation λ.

In figure 1.19, one saw that the condition of compatibility $\overrightarrow{\mathrm{rot}}\,\vec{\chi}_i = 0$ prohibited the singularity by disclination of the field of rotation $\vec{\omega}^{(\varepsilon)}$ deduced from the deformation tensor. Consequently, *if the compatibility condition is no longer zero*, then if $\overrightarrow{\mathrm{rot}}\,\vec{\chi}_i = \vec{\theta}_i \neq \vec{0}$, the course on the closed contour $\boldsymbol{C}$ will result in the existence of a nonzero closure vector $\vec{\Omega}$, called the *Frank vector*. This means from a topological and physical point of view that there will be *discontinuities of rotations by deformation*. The discontinuities $\vec{\Omega}$ are called *disclinations* within the solid lattice.

Concerning the geometro-compatibility equations for 2nd order charges, we can also give an interpretation of the effects of the scalar charges θ of curvature. Indeed, if we consider figure 1.20, we know that the condition of compatibility $\mathrm{div}\,\vec{\chi} = 0$ prohibits the singularity by

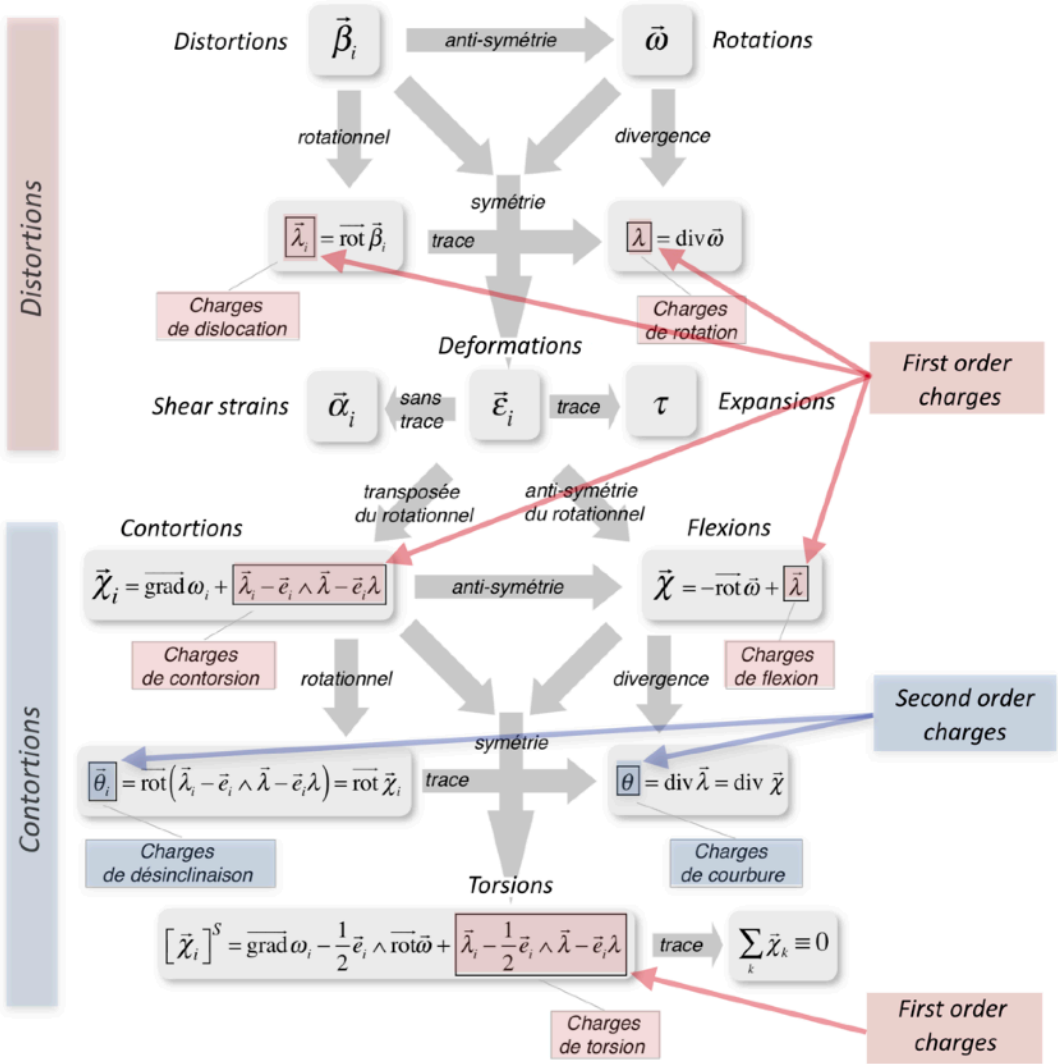

***Figure 2.6** - The system of distortions and contortions in the presence of plastic charges*

divergence of the flexion field, which means that, if $\mathrm{div}\,\vec{\chi} = \theta \neq 0$ within the volume ***V***, it can appear a field of vectors of curvature which diverge, in the same way as the local presence of a density of non-zero electric charges at a place in space induces a diverging electric field.

The operations by symmetry and by vector analysis operators, making it possible to deduce from the tensor charge density $\vec{\lambda}_i$ of dislocation all the charge densities reported in figure 2.6, are summarized in figure 2.7.

It is quite simple to imagine carrying out a macroscopic scale disclination in a solid continuous medium by locally cutting this solid and turning the two jaws of the cut relative to each other, before putting them glue back together. This process is illustrated schematically in figure 2.8 using a pipe of material which is cut according to $\boldsymbol{abcd}$ and which is glued in two different ways:

- either by shearing the plane $\boldsymbol{a'b'cd}$ of one of the jaws without adding or subtracting material (figure 2.8a), which leads to *a unidimensional topological singularity* located on the axis $\boldsymbol{cd}$, called *twist disclination*,

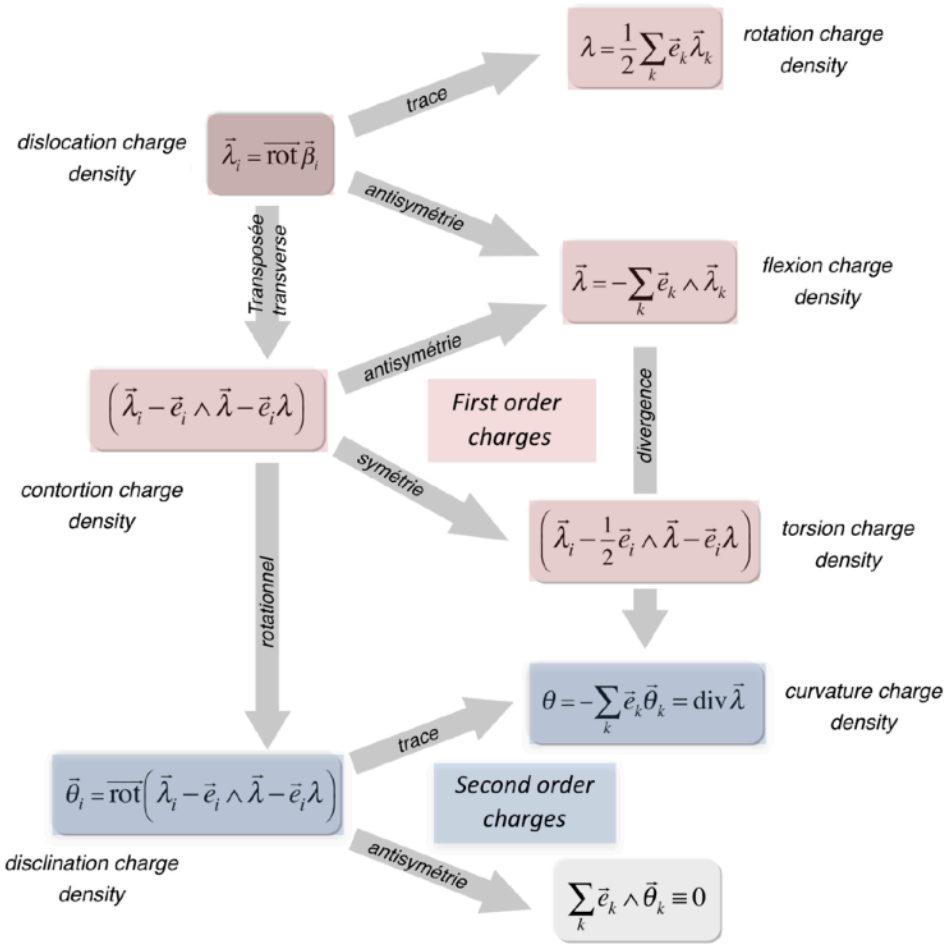

Figure 2.7 - *Deduction of all charge densities from the dislocation charge density*

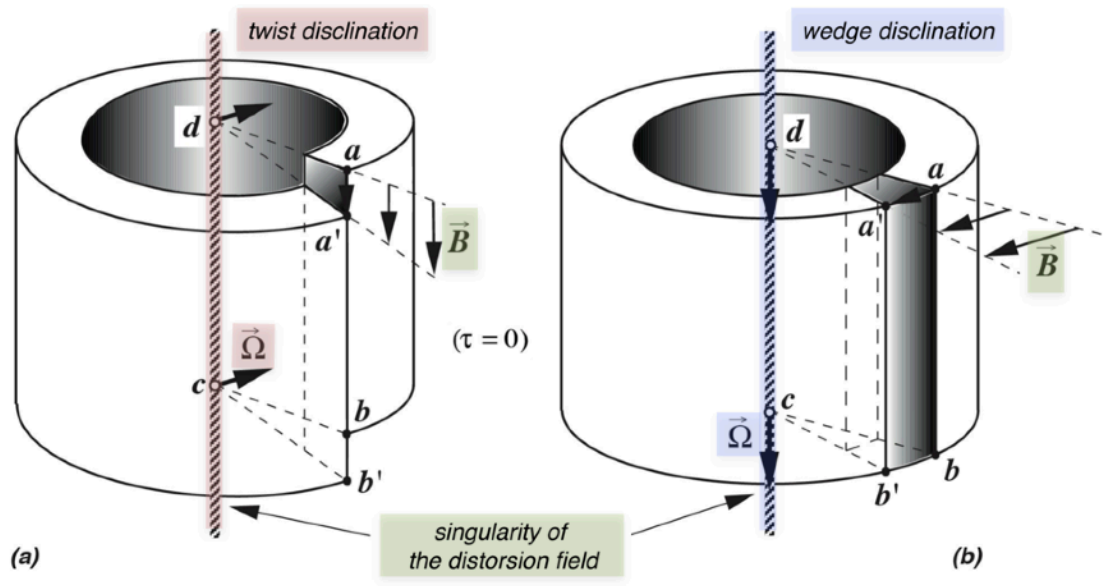

Figure 2.8 - *Realization of twist* ***(a)*** *and wedge* ***(b)*** *disclinations by cutting and gluing*

- either by rotation of one of the interfaces around the edge cd with addition or subtraction of material (figure 2.8b), which leads to *a one-dimensional topological singularity* located on the axis cd, called *wedge disclination.*

Under the condition that the elastic volume expansion τ of the medium remained zero during the plastic deformation process, the vector $\vec{\Omega}$, obtained by the course on the outline C surrounding the singularity, then corresponds exactly to the macroscopic rotation which the jaw $a'b'cd$ underwent. As the vector $\vec{\Omega}$ must remain constant if one varies the diameter of the integration contour C or if one displaces this contour vertically, one deduces that *the charges of disclination must be confined in the immediate vicinity of the axis* cd *of the pipe, and that their tensor density must be a constant along this axis*.

The topological singularities thus obtained are responsible for a distortion field within the solid. Consequently, they require a non-zero formation energy. They are stabilized within the solid by re-bonding the two jaws of the cut, therefore by the bonds within the solid.

By comparing figures 2.2 and 2.8, we can see an astonishing resemblance between screw dislocations and disclinations, as well as between edge dislocations and disclinations. This resemblance is not accidental, since the operations used to generate these discontinuities are very similar. It is interesting to note in particular that the macroscopic disclinations also present a displacement vector $\vec{B}$ going from a to a' (figure 2.8), just like the macroscopic dislocations (figure 2.2). However, this vector $\vec{B}$, in the case of disclintions, increases linearly with the diameter of the integration loop that is used to calculate it. This means that in the presence of a macroscopic disclination, associated with a density of disclinations charges distributed along the

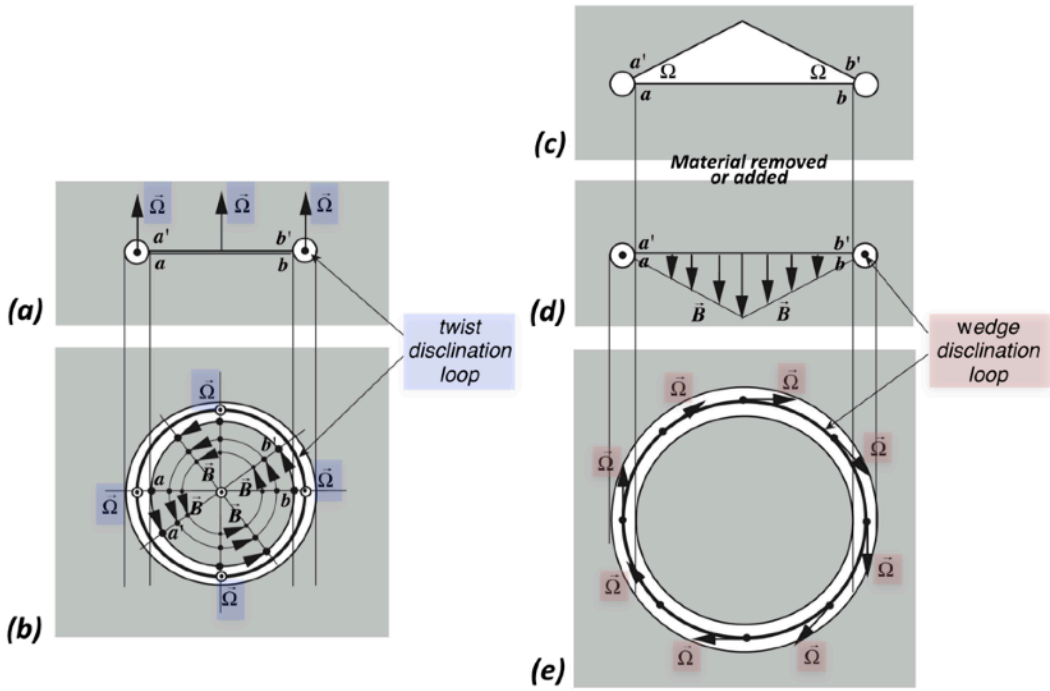

Figure 2.9 - *Realization of a twist disclination loop by rotation of jaws* ***(a)*** *and* ***(b)*** *and a wedge disclination loop by removal (or addition) of a piece of conical material* ***(c)***, ***(d)*** *and* ***(e)***

axis cd of the pipe, there must also exist a density of dislocation charges. But this, instead of being located on the axis of the pipe as it is the case for a macroscopic dislocation, will be found homogeneously *on a surface* located in the cutting plane $abcd$ (figure 2.8), such that the Burgers vector $\vec{B}$ increases linearly with the diameter of the integration loop C.

One can also imagine that within a continuous solid one cuts a void of material in the form of a torus, as illustrated by the section represented in figure 2.4a, then that one cuts the median plane located in the center of the torus. The two jaws ab and $a'b'$ thus formed can then be moved relative to each other, then glued. We can proceed as in figure 2.9a, and move the two jaws in parallel by a rotation $\vec{\Omega}$ of one relative to the other in the cutting plane. After re-bonding, the medium is deformed by rotation $\vec{\Omega}$ and the torus then contains *a macroscopic disclination loop of the twist type*.

Note here that the field of displacement of the medium on either side of the cutting plane is tangential to this plane and that the curvilinear vector of displacement $\vec{B}$ on the cutting plane increases from a zero value in the center to a value maximum on the edges of the torus. At the level of the torus, the local displacement field $\vec{B}$ looks like it can be mistaken for the displacement field of a screw dislocation closed on itself, but it is in fact a *pseudo-dislocation* because *the curvilinear Burgers vector,* tangential to the dislocation line is not preserved in this case, as shown in figure 2.9b.

One could also remove a piece of medium in the center of the torus, of lenticular or conical shape and with an angle Ω at the base, as illustrated in figure 2.9c. In this case, the gluing plane has a local displacement field $\vec{B}$ corresponding to perpendicular Burgers vectors whose lengths have a circular symmetry (figure 2.9d). At the level of the torus, the deformation required for re-bonding is a rotation $\vec{\Omega}$ tangential to the torus, which would therefore correspond to *a macroscopic wedge disclination loop*, but which is in fact *a pseudo-disclination* since the vector of Frank, always tangential to the line of disclination, is not preserved along the line (figure 2.9d).

Quantified dislocations in a lattice

Having described the macroscopic dislocations and disclinations that can appear in a continuous medium, we can now ask ourselves how it is possible to introduce these topological defects on the microscopic scale of a solid lattice. It is clear that the presence of a lattice must necessarily imply a form of quantification of these defects, in the form of topological singularities of the lattice.

It was not until 1934 that the search for this type of singularity in solid lattices really started, and therefore that the theory of lattice dislocations was born, following three famous papers published independently and each describing in its own way the edge dislocation. These are the publications of Orowan[3], Polanyi[4] and Taylor[5]. Then it was in 1939 that Burgers[6] described

---

[3] *E. Orowan, Z. Phys., vol. 89, p. 605,614 and 634, 1934*

[4] *M. Polanyi, Z. Phys., vol.89, p. 660, 1934*

[5] *G. I. Taylor, Proc. Roy. Soc. London, vol. A145, p. 362, 1934*

[6] *J. M. Burgers, Proc. Kon. Ned. Akad. Weten schap., vol.42, p. 293, 378, 1939*

screw and mixed dislocations. And it was finally in 1956 that the first experimental observations of dislocations in metals were reported, simultaneously by Hirsch, Horne and Whelan[7] and by Bollmann[8], thanks to the electron microscope. As for the disclinations, it was in 1904 that Lehmann[9] observed them for the first time in molecular crystals, and it was in 1922 that Friedel[10] gave their first physical description. Then, from the middle of the twentieth century, the physics of defects in solids took on a considerable scale.

As the tensor density $\vec{\lambda}_i$ of dislocation charges must satisfy the conservation equation $\mathrm{div}\,\vec{\lambda}_i \equiv 0$, it is impossible for it to appear in point form and it must be in the form of *three non-diverging vector fields*. This strong condition implies that the tensor density $\vec{\lambda}_i$ of dislocation charges must always occupy *a non-zero volume domain* within the solid medium, which must have a form of *tubular cord*, which has necessarily to cross the solid right through, or have a *shape of an O-ring*.

The area of charges $\vec{\lambda}_i$ of tubular or toric shape can be modeled in the form of *a line of dislocation*, commonly called *dislocation*, representable by *a central one-dimensional fiber* located at the center of the string of non-zero density $\vec{\lambda}_i$ of charges. This *line of dislocation* must then necessarily either cross the solid right through, or form a closed on itself dislocation loop.

The closely related domains of non-zero density of dislocation charges can be modeled in the simplest way in *the form of thin strings*. If the dislocation string is sufficiently thin (of sufficiently small section), the density charge $\vec{\lambda}_i$ can be represented by a single quantity confined to the immediate vicinity of the central fiber of the cord, which will be called *dislocation line*, by introducing the concept of *linear tensor charge* $\vec{\Lambda}_i$ *of dislocation*, namely a set of three vectors defined on the central fiber.

We can then show that the rectilinear strings appearing in a solid lattice are *quantified* on the microscopic scale of the lattice (figures 2.10 and 2.11), and that these strings then represent *elementary plastic singularities* of the distortion fields, in other words *"elementary particles"* of the plastic deformation of the lattice.

If we consider the case of an ordered lattice of particles on a microscopic scale, we can introduce dislocations by cutting the bonds on a lattice plane, parallel displacement of the jaws and reconstruction of the bonds, as illustrated in figures 2.10 and 2.11 in the case of a simple cubic lattice.

The Burgers vector $\vec{\boldsymbol{B}}$ of the singularities thus obtained, that is to say the microscopic discontinuity of the displacements of the lattice due to the presence of the dislocation, is deduced by considering a closed circuit $\boldsymbol{C}$ on the lattice of the real solid, surrounding the singularity, and by searching for the closing vector $\vec{\boldsymbol{B}}$ of the corresponding open circuit *in the undistorted virtual network.*

Thanks to figures 2.10 and 2.11, we can see that the microscopic lattice singularities have an

---

[7] *P. B. Hirsch, R. W. Horne, M. J. Whelan, Phil. Mag., vol. 1, p. 667, 1956*

[8] *W. Bollmann, Phys. Rev., vol. 103, p. 1588, 1956*

[9] *O. Lehmann, «Flussige Kristalle», Engelman, Leibzig, 1904*

[10] *G. Friedel, Ann. Physique, vol. 18, p. 273, 1922*

essential characteristic: *their Burgers vector is quantified*, that is to say that its components $\boldsymbol{B}_i$ can only be integer multiples of the step a of the virtual lattice, thus of the lattice in homogeneous volume expansion of value τ .

The nature of the microscopic plastic singularity can change according to the respective directions which take, in the system of local coordinates, the Burgers vector $\vec{\boldsymbol{B}}$ and the unit vector $\vec{\boldsymbol{t}}$ tangent to the line:

- when $\vec{\boldsymbol{B}}$ is parallel to $\vec{\boldsymbol{t}}$ (figure 2.10), the *linear charge* $\vec{\Lambda}_i$ *of dislocation* presents a non-zero trace ($\Lambda \neq 0$), therefore *a charge of rotation*, and a null antisymmetric part ($\Lambda \neq 0$). One speaks in this case of *screw dislocations*, and of *linear charge* Λ *of rotation of the screw dislocation*, and one symbolically represents this by a screw located on the line of dislocation.

Like $\Lambda = -\vec{\boldsymbol{B}}\vec{\boldsymbol{t}} \,/\, 2$, when the screw dislocation has *a right rotation*, identical to the direction of rotation of a normal screw or a corkscrew, Λ is positive and the vectors $\vec{\boldsymbol{t}}$ and $\vec{\boldsymbol{B}}$ are

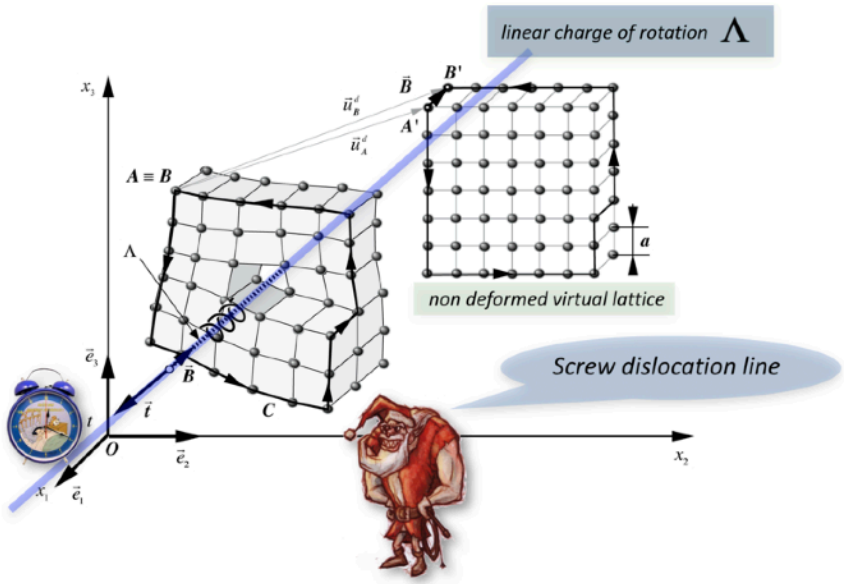

Figure 2.10 - *Screw dislocation line quantified in a cubic lattice*

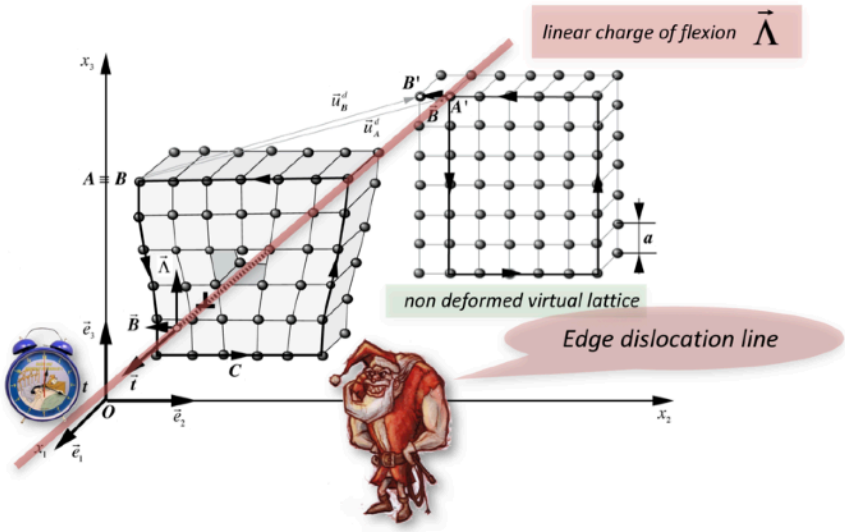

Figure 2.11 - *Edge dislocation line quantified in a cubic lattice*

oriented in opposite directions. On the other hand, if the screw dislocation has *a left rotation*, therefore in the opposite direction of rotation to that of a normal screw or a corkscrew, Λ is negative and the vectors $\vec{t}$ and $\vec{B}$ are oriented in the same direction (figure 2.12) . Note that the choice of a given direction $\vec{t}$ is perfectly arbitrary since only the sign of Λ is fixed.

- when $\vec{B}$ is perpendicular to $\vec{t}$ (figure 2.11), the *linear charge* $\vec{\Lambda}_i$ *of dislocation* presents a null trace ($\Lambda = 0$), therefore no charge of rotation, but a non-zero antisymmetric part ($\vec{\Lambda} \neq 0$). One speaks in this case of *edge dislocations*, and of *linear charge* $\vec{\Lambda}$ *of flexion of the edge dislocation*, and one symbolically represents this one by a sign $\perp$ on the line of dislocation, oriented so as to represent the additional plane of particles. The vector $\vec{\Lambda}$ always has the direction of the additional plane of the edge dislocation (figure 2.13).

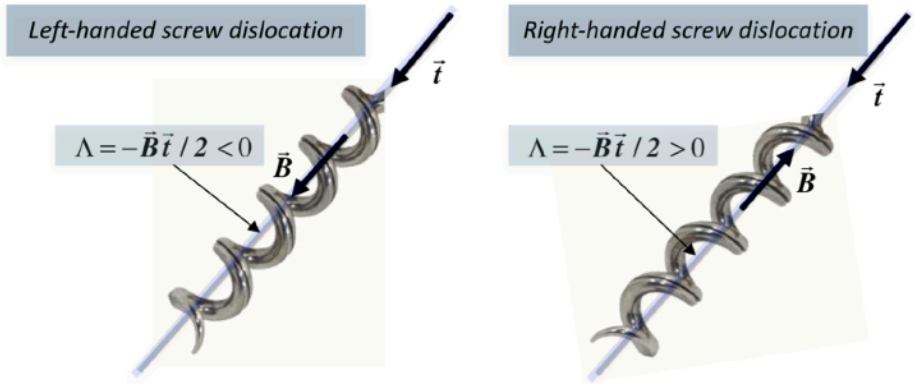

Figure 2.12 - *Burgers vectors of screw type dislocations, «left-handed» and «right-handed» respectively*

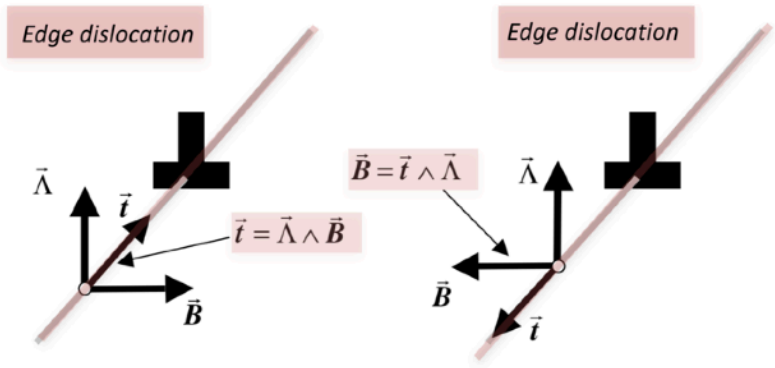

Figure 2.13 - *Burgers vectors of edge type dislocations*

- when $\vec{B}$ is neither parallel nor perpendicular to $\vec{t}$, the *linear dislocation charge* $\vec{\Lambda}_i$ has a non-zero trace ($\Lambda \neq 0$), but also a non-zero asymmetric part ($\vec{\Lambda} \neq 0$), so that it behaves at the same time as a source of elastic and anelastic rotations *and* flexions. We speak in this case of *mixed dislocations*.

In a discrete network, a dislocation can perfectly change direction. In other words, along the dislocation line, the tangent vector $\vec{t}$ is not necessarily preserved. In this case, as the Burgers vector $\vec{B}$ is kept in the local frame, this means that the dislocation must change in nature. For

example, in figure 2.14, a simple cubic lattice model is shown in which a screw dislocation enters the left face, turns becoming mixed within the lattice and emerges as an edge dislocation on the right adjacent face.

Quantified dislocations are the most basic vectors of the plastic deformation of a lattice. In this sense, we could call them the *"elementary particles"* of plastic deformation. Besides, any dislocation string has its *"anti-string"*. Indeed, it is easy to see that two parallel dislocations of the same direction $\vec{t}$ and vectors of Burgers $\vec{B}$ and $-\vec{B}$ respectively annihilate completely if they come to meet within the lattice.

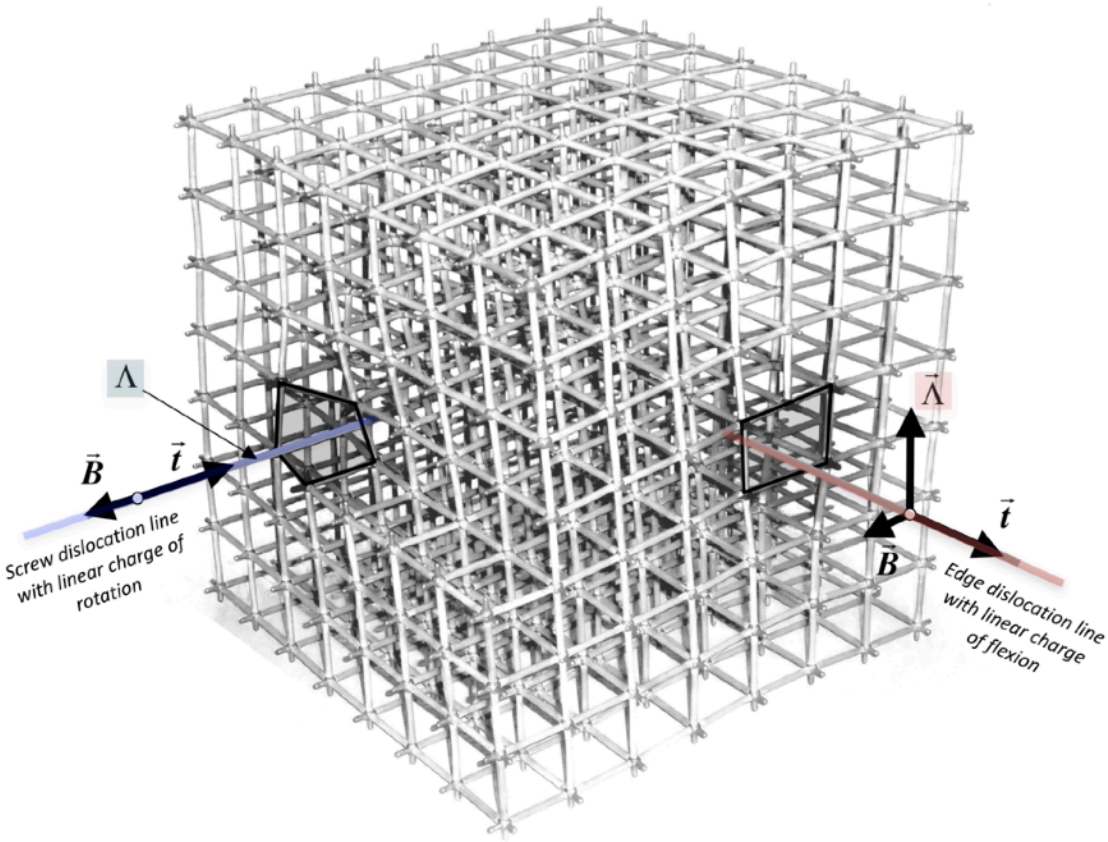

Figure 2.14 - *Dislocation passing from screw to edge type in a cubic lattice*

We also note that screw dislocations, carrying a scalar linear charge $\Lambda \neq 0$, are sources of *a field of divergent local rotations*, which is, as we have seen, the analog of the electric field. So, at a distance $\boldsymbol{R}$ from the string, the norm of the rotation field is simply $|\vec{\omega}| = |\Lambda| / 2\pi\boldsymbol{R}$.

As for the corner dislocations, which carry a fexion charge $\vec{\Lambda} \neq 0$, they are sources of *a lattice flexion*, therefore of *a local curvature of the lattice* in their vicinity as well illustrated by the dislocation emerging from the cubic crystal in the figure. 2.14.

Dissociation of quantified dislocations

The dislocations appearing in structures a little more complex than the simple cubic lattice, such as for example cubic lattices with centered faces, cubic centered or hexagonal, *generally*

present much more complicated core structures. It can thus appear, essentially for energetic reasons, and according to the crystalline system considered, *a dissociation of the core of the dislocation into two or more partial dislocations*, of which the individual Burgers vectors are fractions of the translation vectors of the lattice.

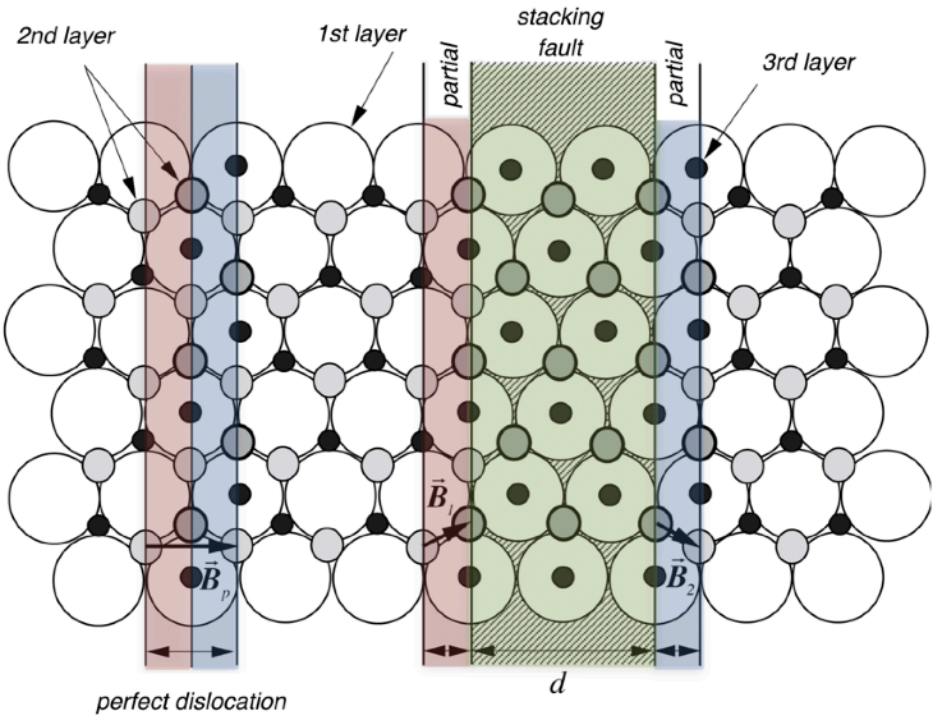

Figure 2.15 - *Dissociation of a perfect dislocation into two partials and a stacking fault ribbon in a face-centered cubic lattice*

For example, in face-centered cubic metals *(CFC)*, the stacking of atoms is characterized by sequences *abc abc abc* ... (figure 2.15). The Burgers vector $\vec{B}_p$ of a perfect dislocation must in principle connect two nodes of the lattice. But for energy reasons, the most favorable Burgers vectors are those that have a minimum length, because the distortion energy stored in the lattice by a dislocation is proportional to the square of its Burgers vector. Thus in the case of figure 2.15, the dislocations have interest to dissociate on their gliding plane in two partial of Burgers vectors $\vec{B}_1$ and $\vec{B}_2$, so that $\vec{B}_p = \vec{B}_1 + \vec{B}_2$. In the case of this dissociation, we have indeed $\vec{B}_1 \vec{B}_2 > 0$, so that $\vec{B}_p^2 = \vec{B}_1^2 + \vec{B}_2^2 + 2\vec{B}_1\vec{B}_1 > \vec{B}_1^2 + \vec{B}_2^2$. The two partial obtained in figure 2.15 by this dissociation are called *Shockley type*. The distance between the two partials is then controlled by a competition between the decrease in energy associated with the increase of the distance between the partials which repel each other, and the increase in energy due to the formation of an energy ribbon of crystalline stacking fault *(abc ac abc abc ...)* located between the two partial dislocations, as shown in figure 2.15.

Since the stacking fault ribbon has an energy γ per unit area, the total energy $E_t(d)$ per unit dislocation length for a dissociated dislocation over a distance d is written $E_t(d) = \gamma d + E_d(d)$, where $E_d(d)$ is the energy of the two partials as a function of the

distance d separating them, which is a monotonic function decreasing from E_0 for $d = 0$ to

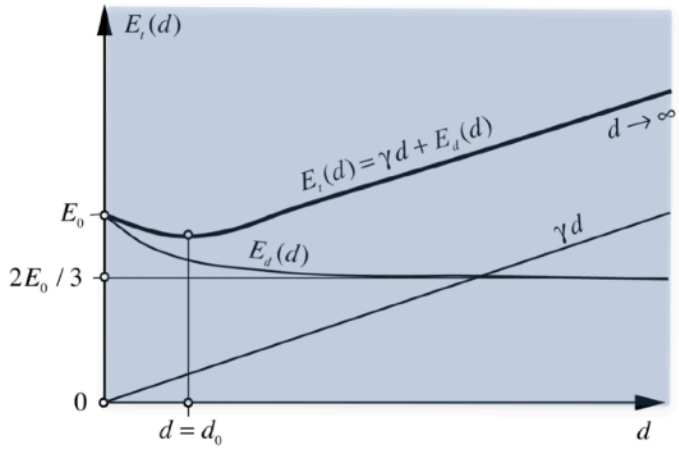

Figure 2.16 - *Total energy of two partial dislocations depending on the distance between them, source of a "strong force" of attraction between them*

$2E_0 / 3$ for $d \to \infty$ in the case of Shockley partials illustrated in figure 2.15.

The energy $E_t(d)$ therefore presents a minimum for the distance $d = d_0$ (figure 2.16), which is the equilibrium distance between the two partials, controlled by the competition between the energy decrease associated with the distance increase between the repulsive partials, and the energy increase due to the formation of a stacking-fault ribbon between the two partials. We see here appear a behavior of the energy $E_t(d)$ which induces an interaction force between the two partial which one could qualify as *"strong force"*, in the sense that the energy of the pair of partial presents a minimum which fixes the equilibrium position d_0 , but that it continues to increase if we try to increase the separation distance beyond d_0 . The qualifier *"strong force"* is proposed here because the attractive behavior of the interaction force between partial at long distance presents a very interesting analogy with the strong force acting between quarks in the Standard Model of elementary particles.

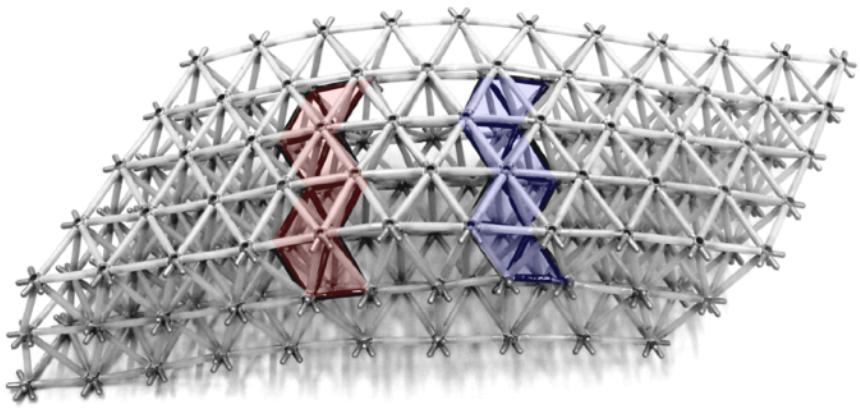

Figure 2.17 - *Model of a mixed dislocation in a face centered cubic lattice presenting a dissociation into two partials, as well as kinks on the two partial dislocations*

By way of exemplary illustration, figure 2.17 shows the model of a mixed dislocation, with an edge and a screw nature at the same time, dissociated into two partials in a cubic face centered structure. We can clearly see the existence of a stacking defect between the two partials. And since this is a mixed dislocation, the two partials show a series of kinks in it. In addition, we can even observe the bending of the network induced by the edge part of the dissociated dislocation.

All of the consequences linked to the structure of the lattice are obviously too specific for each conceivable crystal structure to be dealt with in detail here. But they can be approached in any book dealing with dislocations in crystalline structures.

Quantified dislocation membranes

A thin interface which contains dislocation charges and which separates two media containing no charges is called *a charged membrane*. These membranes can be any surfaces in space *(infinite surfaces, closed spheroidal or toric surfaces, ribbons or hollow tubes, thin plates, etc.)*, with the only topological condition that, on any point of the membrane, the equation of conservation of the dislocation charges $\mathrm{div}\,\vec{\lambda}_i \equiv 0$ is satisfied and that the disclination charges derive from the dislocation charges through the relation $\vec{\theta}_i = \overrightarrow{\mathrm{rot}}\left[\vec{\lambda}_i - \vec{e}_i \wedge \vec{\lambda} - \vec{e}_i \lambda\right]$.

If a dislocation charged membrane is very thin, it is possible to introduce the notion of *surface tensor charge* $\vec{\Pi}_i$ *of dislocation*. The existence of a *surface charge of dislocation* $\vec{\Pi}_i$ in the membrane leads to a discontinuity of the tangential components of the distortion vectors $\vec{\beta}_i$ on either side of it, and it is subject to the condition that *there is a gradient of the components of the Burgers vector on the surface of the membrane*.

Two-dimensional modeling of a thin membrane obtained with surface charges is generally called *a joint*. The joint is then entirely characterized by the data of the surface tensor $\vec{\Pi}_i$ of dislocation charges, the vectors of which are *tangent to the surface of the membrane*, which is in fact a direct consequence of the equation of conservation $\mathrm{div}\,\vec{\lambda}_i \equiv 0$ of the dislocation charges. But it can also be characterized by the data of the anti-symmetrical part $\vec{\Pi}$ (the surface charge of flexion of the joint) and of the trace Π (the surface charge of rotation of the joint) of the load tensor $\vec{\Pi}_i$, as in the case of the one-dimensional lines of dislocation. This point is perfectly illustrated in figure 2.18, in which three thin membranes are presented whose Burgers vectors, growing linearly along the axis $\boldsymbol{O}x_1$, are oriented respectively along the axes $\boldsymbol{O}x_3$, $\boldsymbol{O}x_1$, and $\boldsymbol{O}x_2$. Since these thin dislocation membranes actually disorient or accommodate the solid grains on either side of the membrane, they are generally called *grain boundaries*.

We can for example consider that these membranes are in fact charged by edge dislocations or screw dislocations oriented parallel to the axis $\boldsymbol{O}x_2$. We can then simply represent each individual dislocation by a linear vector charge $\vec{\Lambda}$ if it is an edge dislocation or by a scalar linear charge Λ if it is a screw dislocation. We then verify that:

- the thin edge type membrane with a Burgers vector perpendicular to the surface and increasing along the axis $\boldsymbol{O}x_1$ (figure 2.18a) can be entirely characterized by a *vector surface charge* $\vec{\Pi}$ *of flexion*, the vector of which is tangent to the plane of the membrane, directed according to $\boldsymbol{O}x_1$, and worth $\vec{\Pi} = \vec{\Lambda} / \boldsymbol{d}$. As this type of edge membrane makes it possible to disorient the solid grains located on either side of the membrane, it is called *a disorientation*

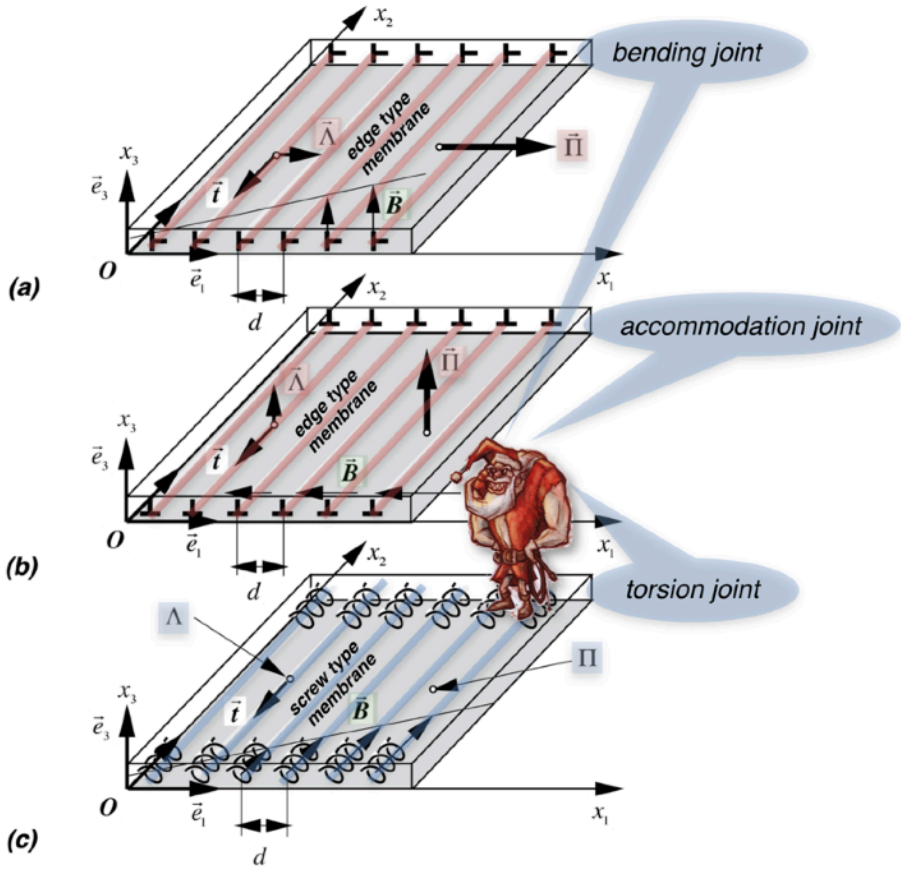

Figure 2.18 - *Edge type dislocation membranes: bending joint* ***(a)*** *and accommodation joint* ***(b)*** *or screw type dislocation membranes: torsion joint* ***(c)***

joint, and in this particular case, as the disorientation corresponds to a flexion of the solid, we speak of *a bending joint*.

- the thin edge-type membrane with a Burgers vector parallel to the surface and increasing along the axis $\boldsymbol{O}x_1$ (figure 2.18b) can be entirely characterized by a *vector surface charge* $\vec{\Pi}$ *of flexion*, whose vector is perpendicular to the membrane, and being equal $\vec{\Pi} = \vec{\Lambda} / \boldsymbol{d}$. As this type of edge membrane in fact makes it possible to modify in the direction $\boldsymbol{O}x_1$ the density of the crystalline planes of the solid grains situated on either side of the membrane, it can be qualified as *an accommodation joint*.

- the thin screw type membrane with a Burgers vector parallel to the membrane and increasing along the axis $\boldsymbol{O}x_1$ (figure 2.18c) is entirely characterized by the *scalar surface charge* Π *of rotation,* being equal $\Pi = \Lambda / \boldsymbol{d}$. This type of screw membrane also corresponds to a disorientation joint between the solid grains located on either side of the membrane. In this particular case, as the disorientation corresponds to a rotation of the grains relative to one another, we speak of *a torsion joint*.

Quantified disclinations in a lattice

As the charges of disclination always derive from dislocation charges through relationship $\vec{\theta}_i = \overrightarrow{\mathrm{rot}}\left[\vec{\lambda}_i - \vec{e}_i \wedge \vec{\lambda} - \vec{e}_i \lambda \right]$, *there can be no dislocation strings in an isolated state*. But strings

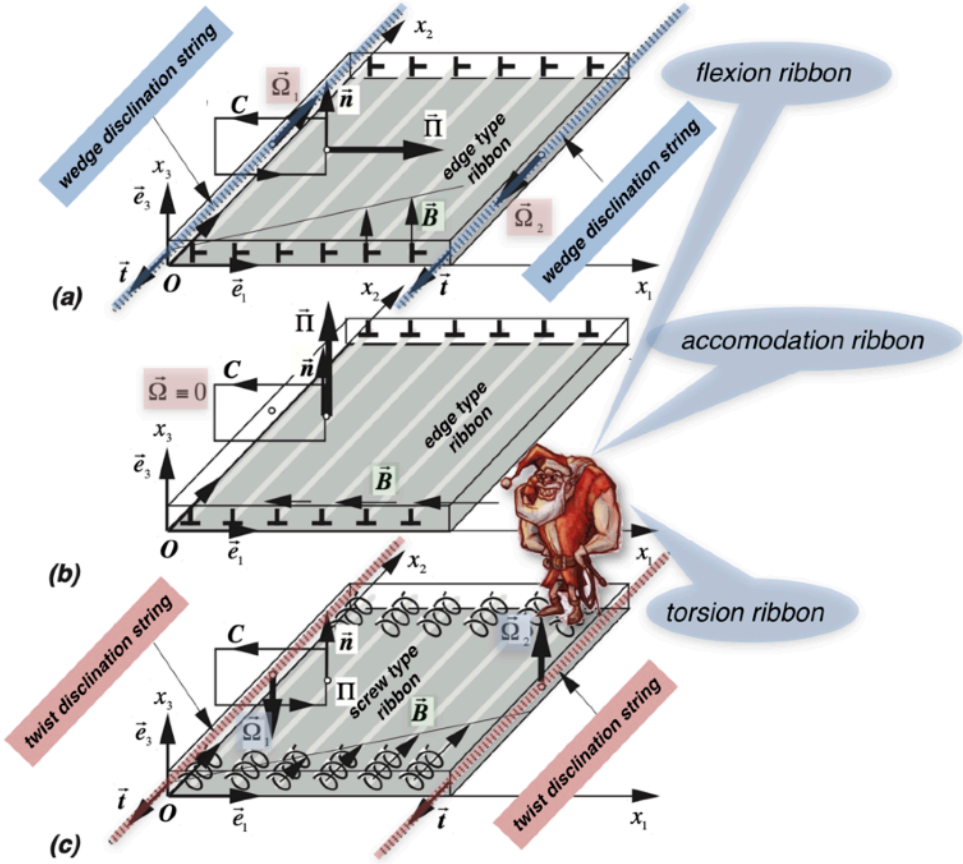

Figure 2.19 - *Dislocation ribbons bordered by disclination lines of wedge type* ***(a)*** *and twist type* ***(c)****. The dislocation ribbon* ***(b)*** *is not bordered by disclination lines*

of disclination can appear *in the presence of a large dislocation charge domain, such as a dislocation membrane in the form of a ribbon*.

We can consider for example the case of flat ribbons charged with dislocations, which abruptly stop along the axis Ox_1, as shown in figure 2.16. The boundaries which border these dislocation ribbons are then lines of disclination, because it appears on these boundaries singularities by disclination of the field of rotations by deformations, as described in figure 1.19, having a non-zero Frank vector $\vec{\Omega}$. In this figure, we see the following points:

- the edge-type dislocation ribbon with a Burgers vector perpendicular to the membrane and increasing along the axis Ox_1 (figure 2.19a) corresponds to *a localized bending joint*. It is bordered by two wedge type disclinations whose Frank vectors are parallel to the axis Ox_2, and which are respectively worth $\vec{\Omega}_1 = -\vec{\Omega}_2 = -\vec{\Pi} \wedge \vec{n} = -\left|\vec{\Pi}\right| \vec{t}$,
- the edge-type dislocation ribbon with a Burgers vector parallel to the membrane and increasing along the axis Ox_1 (igure 2.19b) corresponds to *a localized accommodation joint*. As there is then no discontinuity in the rotational field by deformations, it is not bordered by any disclination and $\vec{\Omega}_1 = \vec{\Omega}_2 \equiv 0$,
- the screw-type dislocation ribbon with a Burgers vector parallel to the membrane and increasing along the axis Ox_1 (figure 2.19c) corresponds to *a localized torsional joint*. It is

bordered by *two twist-type disclinations* whose Frank vectors are parallel to the axis Ox_3, and which are worth respectively $\vec{\Omega}_1 = -\vec{\Omega}_2 = -\Pi\vec{n}$.

It will be noted that the disclination of figure 2.19a corresponds to the macroscopic disclination represented in figure 2.8b, while that the disclination of figure 2.19c corresponds to the macroscopic disclination of figure 2.8a. The quantification on a cubic lattice of a ribbon of disclination similar to that of figure 2.19c is illustrated in figure 2.20, in which one has reported the two disclinations bordering a quantized dislocation ribbon composed of three aligned lattice screw dislocations.

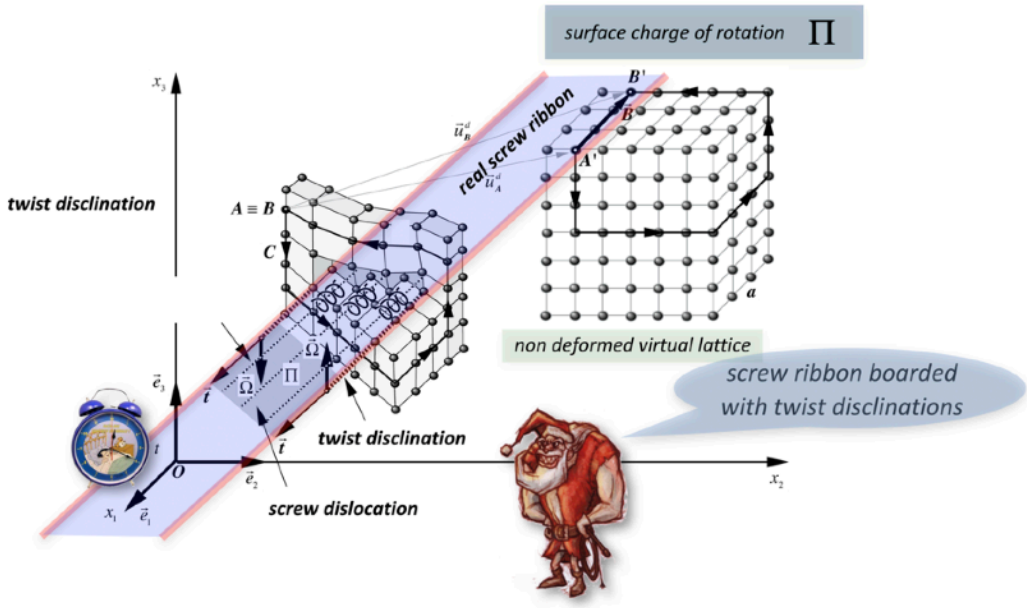

Figure 2.20 - *Quantized two-dimensional dislocation ribbon composed of three screw lattice dislocations*

Although there cannot be isolated disclinations, it is possible to imagine structured solid media which would contain rectilinear disclinations quantified on their lattice in the case of wedge disclinations, as shown in figure 2.21. In this figure, we have represented two wedge disclinations with Frank vectors $\Omega = \mp 90°$ in a simple cubic lattice, and we have also reported the curvature vector $\vec{\chi}$ due to the charge Θ.

We can then imagine that there could be different families of quantified wedge disclinations by considering solid media with different arrangements of the particles in a secant plane of the disclination line. For the example, we will consider here simple arrangements like the arrangement on a quadratic network. But we could obviously also consider more complex arrangements, such as three-dimensional centered cubic, hexagonal or face centered cubic structures.

In the case of a quadratic arrangement, there can exist at most 3 different quantified wedge disclinations, which will be called $C1$, $C2$ and $C3$, with angles of rotation Ω of + 90 °, + 180 ° and + 270 °, to which correspond 3 quantified wedge anti-disclinations, $\bar{C}1$, $\bar{C}2$ and $\bar{C}3$, with rotation angles of -90 °, -180 ° and -270 ° (figure 2.22).

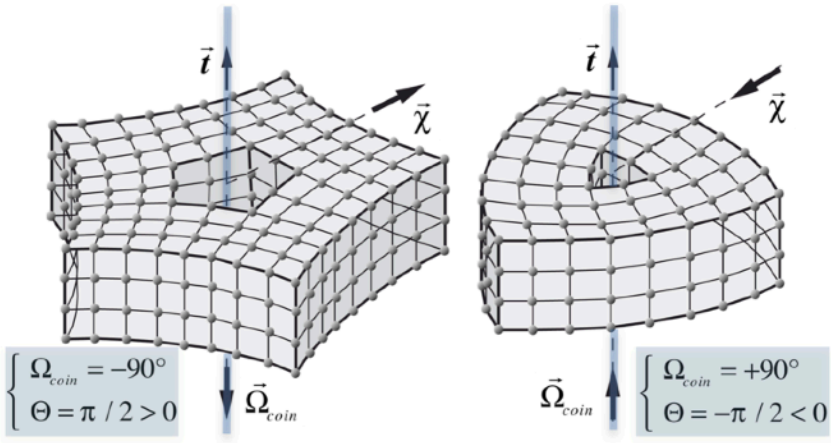

Figure 2.21 - *Examples of quantified wedge disclination* $\Omega = \mp 90°$ *in a simple cubic lattice*

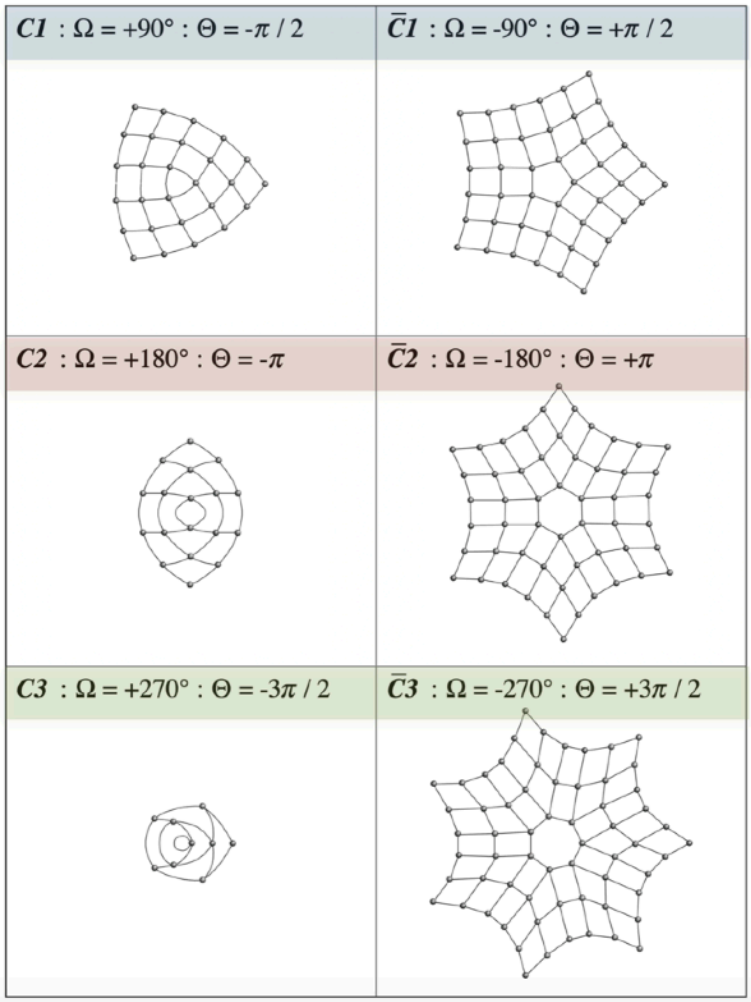

Figure 2.22 - *Family of quantified wedge disclinations in a quadratic planar arrangement*

In the case of figures 2.22, we have reported the disclinations with a calculated size so that the volume expansion τ is identical in all the figures. Note also that the tilt of + 270 ° in the quadratic arrangement could exist or not exist depending on the imaginary medium considered, because their existence is linked to the possibility of connecting two bonds of the same "particle" in the solid structured medium that we consider.

It has been shown that there cannot be isolated disclinations with non-zero Frank vector. Consequently, it is necessary to combine several disclinations close to one another so that the Frank vector obtained on a contour surrounding all these disclinations is zero.

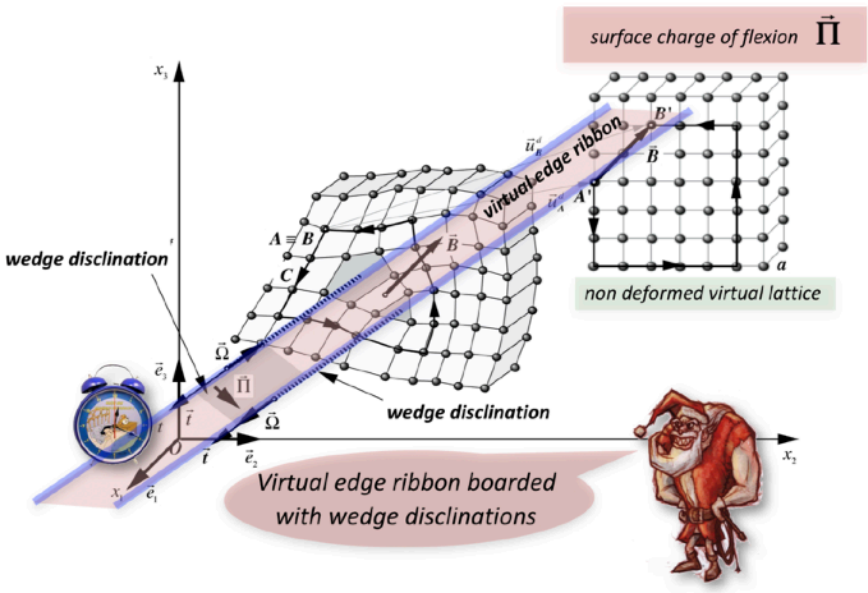

Figure 2.23 *- Doublet of quantified wedge disclinations with virtual edge dislocation ribbon*

The example shown in figure 2.23 illustrates this fact perfectly: by coupling two quantified wedge disclinations of type $C1$ and $\bar{C}1$ in a simple cubic structure, the total Frank vector becomes zero, and a virtual edge dislocation ribbon appears between the two disclinations, of non-zero global Burgers vector $\vec{B}$. The edge-type dislocation ribbon is similar to that shown in figure 2.19a and therefore contains a vector surface charge $\vec{\Pi}$ of flexion. But this real flexion charge $\vec{\Pi}$ is not associated with real quantized dislocations of the lattice, but *with a virtual ribbon of edge dislocation*. In the case of this wedge disclination doublet, it is fairly easy to imagine that the distortion energy increases extremely quickly if the two disclinations are moved away, so that these two disclinations can be considered to be linked by a *"strong force"*, that is to say an attractive force which increases when an attempt is made to distance the two disclination.

We can find the multiplets of zero Frank vector disclinations which it is possible to construct on the basis of the quantified wedge disclinations that we have described in the case of the simple quadratic lattice. The basic zero vector Frank multiplets, i.e. those which can no longer be further decomposed into two or more zero Frank vector multiplets, are shown in figure 2.24. We note that, in a simple quadratic lattice, there can exist 3 doublets, 4 triplets and 2

quadruplets.

In table 2.24, the multiplets composed with disclinations $C3$ of + 270 ° are grayed out, because they might not exist, for example in structured media which do not allow two bonds of the same "particle" to be connected together.

3 doublets
+90° / -90°
+180° / -180°
+270° / -270°

4 triplets	
+90° / +90° / -180°	*-90° / -90° / +180°*
+90° / +180° / -270°	-90° / -180° / +270°

2 quadruplets	
+90° / +90° / +90° / -270°	-90° / -90° / -90° / +270°

Figure 2.24 - *The multiplets of quantified wedge disclinations in a quadratic planar structure*

Solid lattices with axial symmetry

Mixed strings resulting from *the combination of a string or a line of disclination with a string or a line of dislocation* are called *strings or lines of dispiration*, or simply *dispirations*. Note that the term "dispiration" is an Anglicism and that there is no French translation of this term.

One can imagine lattices which have a certain axial symmetry of the particles composing it, like the cubic networks ***(a)*** and ***(b)*** illustrated in figure 2.25. This axial symmetry of the particles can simply present a privileged direction of the particles in the planes of the structure, as in case ***(a)***, which has an alternating structure of successive layers ***a***, ***b***, ***a***, ***b***, ***a***, ***b***,… The axial symmetry can also have a preferential direction and way as in case ***(b)*** which has an alternating structure of successive layers ***a***, ***b***, ***c***, ***d***, ***a***, ***b***, ***c***, ***d***, ...

Moreover, in case ***(b)***, the direction of rotation of the axes of the particles along the vertical axis produces an oriented medium, which is qualified as right-handed (clockwise) in case ***(b)*** illustrated in figure and left-handed (counter-clockwise) in the case where the planes rotate in the opposite direction.

If it is forbidden to break the axial orientation of the particles in a plane, it is not possible to introduce a vertically oriented screw dislocation with any Burgers vector. Indeed, if the distance between the horizontal planes is worth a , in order to ensure the continuity of the orientation of the particles, and also of their direction in the case ***(b)***, it is necessary that the length of the vector of Burgers $\vec{B}_{vis}$ of the dislocation vis is equal to $\pm 2a$ in case ***(a)***, and $\pm 4a$ in case ***(b)***.

In media with axial symmetry such as those shown in figure 2.25, we have just explained that the screw dislocations must have Burgers vectors $\vec{B}_{vis}$ whose lengths are multiples of the

length of the lattice pitch. In this case, the screw dislocations may have an interest in splitting into partial with Burgers vectors of length a, forming respectively 2 or 4 partial in cases ***(a)*** and ***(b)*** respectively. Between the partial dislocations, *ribbons of connection faults* are formed between axial planes ***ab***, ***bc***, ***cd***, etc. The partial separation distance then depends on the energy γ per unit area of the connection fault.

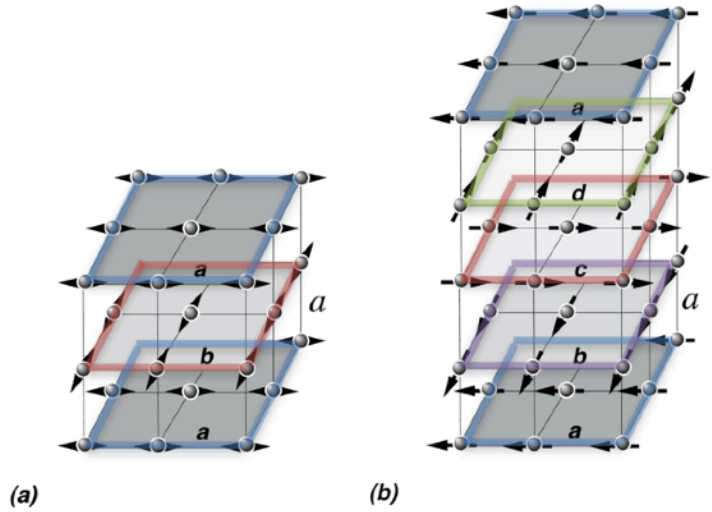

Figure 2.25 - *Cubic lattices with axial symmetry, simple in case* ***(a)****, and oriented of dextrorotatory type (right-handed) in* ***(b)***

If the connection fault ribbon has an energy γ per unit area, the total energy $E_t(d)$ per unit length of a dissociated screw dislocation over distances d is written:

- $E_t(d)=\gamma d+E_d(d)$ in case ***(a)***, where $E_d(d)$ is the energy of the two partials as a function of the distance d separating them, which is a monotonic function decreasing from E_0 for $d=0$ to $E_0/3$ for $d\to\infty$,
- $E_t(d)=3\gamma d+E_d(d)$ in case ***(b)***, where $E_d(d)$ is the energy of the four partials as a function of the distance d separating them, which is a monotonic function decreasing from E_0 for $d=0$ to $E_0/3$ for $d\to\infty$.

The energy $E_t(d)$ therefore has a minimum similar to that shown in figure 2.16 for the distance $d=d_0$, which is the equilibrium distance between the two or the four partial, controlled by the competition between the decrease in energy associated with the increase in distance between the partials and the increase in energy due to the formation of an energy ribbon due to lack of connection between the partials. This behavior of the energy $E_t(d)$ induces a force of interaction between the partials which one can quite qualify as *strong force*, in the sense that the energy of the triplet of partials will increase if one tries to increase the distance of separation beyond d_0. This strong force therefore presents in its behavior an interesting analogy with the strong force acting between quarks in the Standard Model of elementary particles.

We can immediately imagine that there must also be connection conditions ensuring the continuity of the axial symmetry if we want to introduce a disclination in such a network. In fact, to ensure this continuity, it will necessarily be associated with the disclination a screw dislocation with the correct Burgers vector $\vec{\boldsymbol{B}}$. It therefore appears here a structural necessity to

introduce dispirations in such environments.

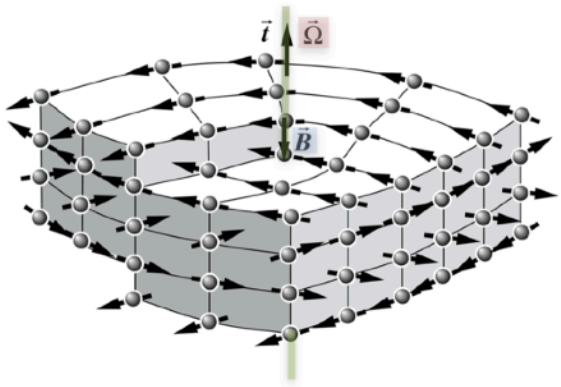

Figure 2.26 - *Dispiration of + 90 ° introduced into the axial lattice of figure 2.25 (b) showing the need to add a translation vector* $\vec{B}$ *to ensure axial continuity*

Figure 2.26 illustrates this point perfectly. Indeed, to introduce an disclination Ω =+90 ° in the medium represented in figure 2.25*(b)*, it is necessary to add to it a correctly oriented screw dislocation, of Burgers vector $\vec{B}$ and of length a , which ensures the continuity of the axial orientation of the particles on the planes of the medium.

Note that screw dislocation of Burgers vector of opposite direction and length $3a$ could also have ensured the continuity of the axial orientation of the particles on the planes of the medium, so that there are two different dispitations with rotations Ω =+90 °, both with a linear charge of

	Θ	$\Lambda_{(a)}$	$\Lambda_{(b)}^{(dextrogyre)}$	$\Lambda_{(b)}^{(lévogyre)}$
vis	0	$\pm 2a$	$\pm 4a$	$\pm 4a$
C1	$-\pi / 2$	$\pm a$	$+a\ , -3a$	$-a\ , +3a$
$\bar{C}1$	$+\pi / 2$	$\pm a$	$-a\ , +3a$	$+a\ , -3a$
C2	$-\pi$	$0\ , \pm 2a$	$+2a\ , -2a$	$+2a\ , -2a$
$\bar{C}2$	$+\pi$	$0\ , \pm 2a$	$+2a\ , -2a$	$+2a\ , -2a$
C3	$-3\pi / 2$	$\pm a$	$-a\ , +3a$	$+a\ , -3a$
$\bar{C}3$	$+3\pi / 2$	$\pm a$	$+a\ , -3a$	$-a\ , +3a$

Tableau 2.27 - *Linear charges of curvature* Θ *and rotation* Λ *of the dispirations in the cubic structures of figure 2.25* ***(a)*** *and* ***(b)***

curvature of $\Theta = -\pi / 2$, but differentiated by their Burgers vector $\vec{B}$ associated with a linear charge of rotation Λ being equal to $\Lambda = a$ or $\Lambda = -3a$.

It is not too difficult to find out which linear torsion charges Λ should be associated with the different wedge dispirations of linear charge of curvature Θ that can be introduced into the cubic structures shown in figure 2.25.

In Table 2.27, these loads are reported for the cubic structures of figures 2.25***(a)*** and ***(b)***. In case ***(a)***, the structure shows no difference between *a righthanded orientation* and *a lefthanded orientation* of the particles in the lattice. On the other hand, there appears to be a difference between these two orientations in case ***(b)***, which implies a change in sign of the charge Λ between the *righthanded* and *lefthanded* environments.

Quantified dislocation and disclination loops in a lattice

To satisfy the conservation equation $\mathrm{div}\,\vec{\lambda}_i = 0$, a dislocation or a disclination string cannot be abruptly interrupted within the medium. On the other hand, such a string closing on itself to form a localized loop always satisfies the conservation equation. In this section, we will therefore present this type of loops as well as their properties in a solid lattice.

For a circular dislocation loop of radius R, the tensor linear charge $\vec{\Lambda}_i$ of the dislocation can be related to its Burgers vector using the relation $\vec{\Lambda}_i = -\vec{t}\,\boldsymbol{B}_i$ where $\vec{t}$ represents the unit vector tangent to the dislocation line.

Three types of dislocation loops then appear according to the orientation of the Burgers vector with respect to the normal $\vec{n}$ to the surface of the loop, as shown in Figure 2.28:
- the *slip loops* (figure 2.28a) when $\vec{B} \perp \vec{n}$, having both edge portions (where $\vec{B} \parallel \vec{m}$)), screw portions (where $\vec{B} \parallel \vec{t}$) and mixed portions. Their Burgers vector can take any orientation in the plane perpendicular to $\vec{n}$. They are obtained by the process described in figure 2.4b,

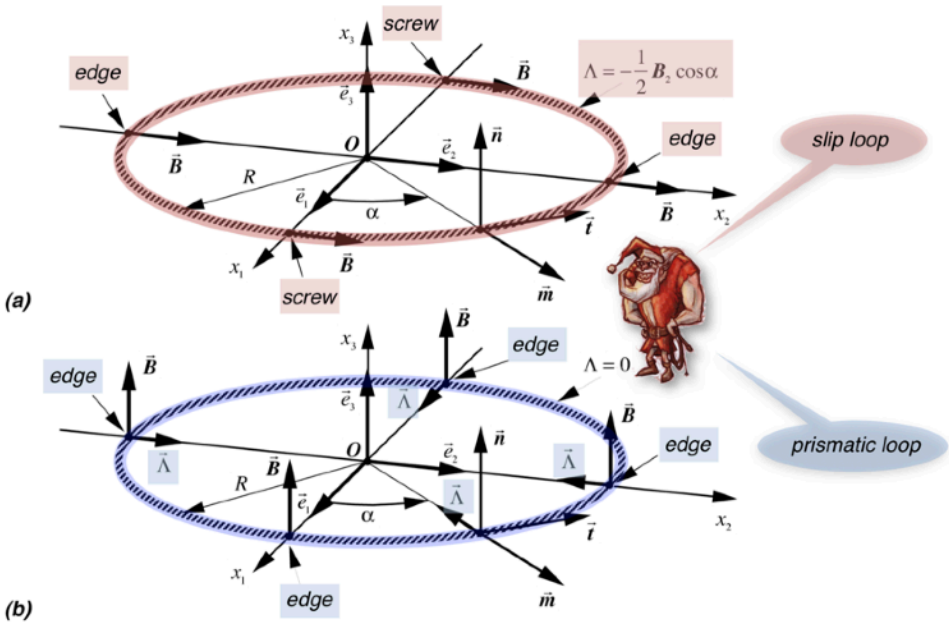

Figure 2.28 - *Slip dislocation loop* ***(a)*** *and prismatic dislocation loop* ***(b)***

- the *prismatic loops* (figure 2.28) when $\vec{B} \parallel \vec{n}$, which have their Burgers vector in the imposed direction of the unit vector $\vec{n}$ perpendicular to the plane of the loop, and which are obtained by the process described in figure 2.4c and d.
- the *mixed loops* when $\vec{B}$ has a component in the direction of $\vec{n}$ and a component in the plane of the loop.

We will see later that it is useful to introduce the notions of *global scalar charges of rotation* q_λ and *global scalar charges of curvature* q_θ, which will in fact be very important for characterizing the topological effects at long distance of topological singularities. These global scalar charges are perfectly analogous to the electrical charge of an electron, for example.

We can define a *global scalar charge* q_λ *of rotation* of a dislocation loop as the integral (the sum) of its *scalar linear density* Λ *of torsion charge* taken on the contour of the loop:
- in the case of the prismatic loop (figure 2.28b), the *global scalar charge* q_λ is null because the linear density Λ of torsion load is null everywhere on the contour of the loop.
- in the case of the slip loop (figure 2.28a), the linear density Λ of torsion charge evolves along the loop according to the cosine of the angle α, becoming positive, null, negative and null on a complete turn, so that the global scalar charge q_λ of rotation is also zero ($q_\lambda = 0$) for this type of loop. On the other hand, as the linear density Λ of torsion charge is positive for $\alpha = 0$ and negative for $\alpha = 180°$ in the case of *the slip dislocation loop* shown in figure 2.28a, we deduce that the slip dislocation loops have *a dipolar momentum of rotation charges*.

We can also define a *global scalar charge* q_θ *of curvature* of a dislocation loop as the integral (the sum) of its scalar linear density Θ of curvature charge taken on the contour of the loop:

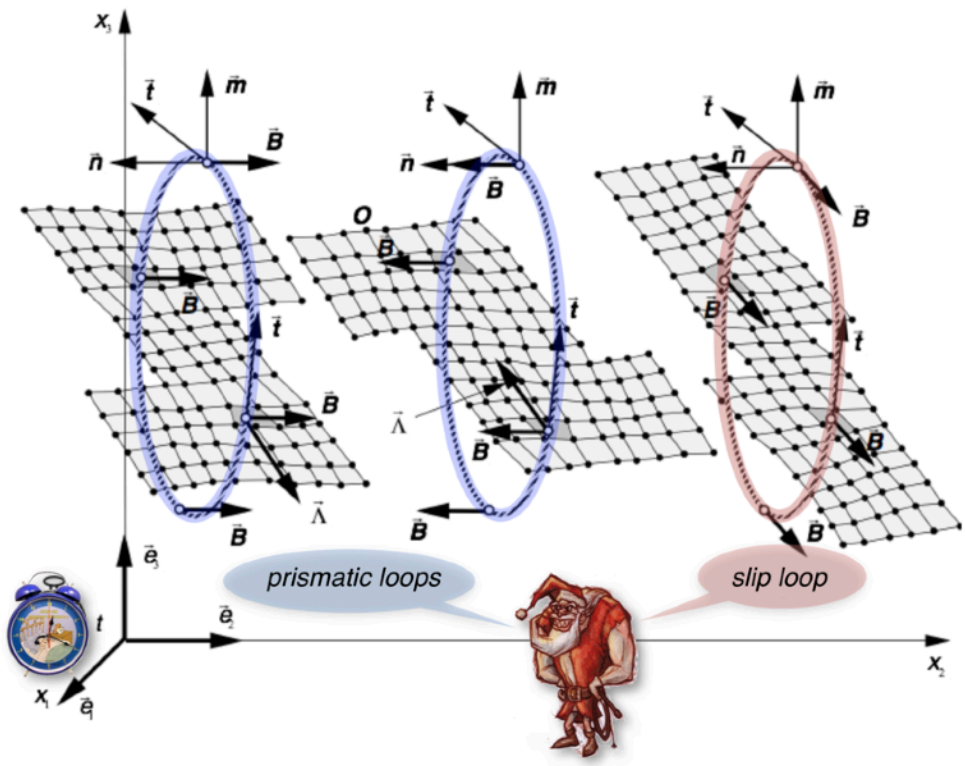

Figure 2.29 - *Quantified loops of dislocations in a cubic lattice*

- in the case of *the slip loop* (figure 2.28a), as the linear density Θ of curvature charge is null all along the loop, *its total scalar charge* q_θ *of curvature is null.*
- in the case of *the prismatic loop* (figure 2.28b), the linear density Θ of curvature charge is not zero and is worth $\Theta = -\vec{n}\vec{B} / R$, so that the *total scalar charge* q_θ *of curvature of the prismatic loop is worth* $q_\theta = -2\pi\vec{n}\left(\vec{t} \wedge \vec{\Lambda}\right) = 2\pi\vec{\Lambda}\vec{m}$

At the microscopic scale of a solid lattice, the Burgers vector of dislocation loops are quantified, as shown schematically in figure 2.29 for two prismatic loops and for one slip loop within a cubic network. In this figure, we also clearly observe the following facts:
- the prismatic dislocation loops are obtained by adding or removing a plane of particles within the loop (translation perpendicular to the plane of the loop), so that the network presents *"extra-matter"* on the plane of the loop; note that the overall scalar charge q_θ of divergent curvature of the prismatic loop is directly linked to the existence of this *"extra-matter"*,
- the slip dislocation loops are obtained by sliding (translation parallel to the plane of the loop) in the direction of the Burgers vector, so that the lattice does not present any "extra-matter" in this case. On the other hand, the presence of a screw component in the regions where $\vec{B} \,||\, \vec{t}$ induces *a dipolar field of rotation in the vicinity of the slip loop*.

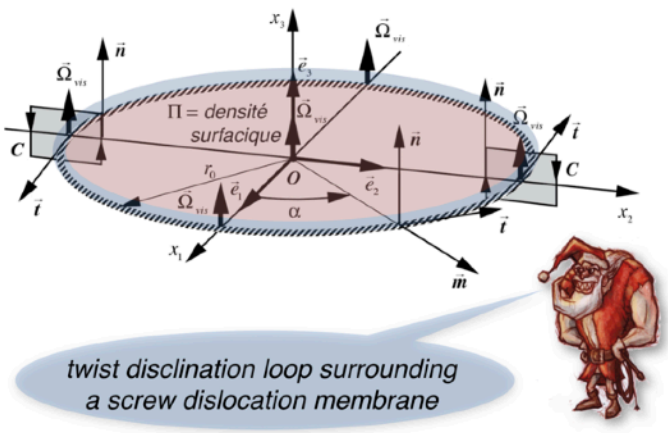

Figure 2.30 - *Twist disclination loop with its charged membrane*

In Figure 2.9, we have shown the macroscopic realization of a screw disclination loop. But what are its main characteristics? For this, consider a loop consisting of a screw disclination generated by a rotation $\vec{\Omega}_{vis}$ of the upper plane by an angle α relative to the lower plane, as shown in figure 2.30. The fact that two planes which have been displaced relative to one another are glued together within the loop must show on the plane of the loop a surface charge Π of dislocation. On the contour of this surface charge, a twist disclination loop appears, the Frank vector of which is directly linked to the surface charge Π of dislocation because $\vec{\Omega}_{vis} = -\vec{n}\Pi$, which is itself linked to the angle of rotation $\alpha = \Omega_{vis} = -\Pi$ imposed on the two jaws.

The surface charge Π of rotation rotation can be integrated (summed) on the surface of the loop, and there then appears a global charge q_λ *of* rotation of such a loop, which is worth

$\boldsymbol{q}_\lambda = \pi R^2 \Pi$. This global charge $\boldsymbol{q}_\lambda$ is actually the rotation charge of the twist disclination loop as seen from a long distance from the loop. This means that such a loop can behave as the source of a divergent field $\vec{\omega}$ of rotation within the solid medium.

Note that it is possible to see a disclination loop somewhat differently. Indeed, the fact of carrying out the rotation of the two planes one with respect to the other induces a displacement along the string *similar to that of a screw dislocation.* The Burgers vector and the linear charge of this *screw pseudo-dislocation* would then be worth $\Lambda_{vis} = -\vec{\boldsymbol{B}}_{vis}\vec{\boldsymbol{t}}/2 = R\Pi/2$, so that the global charge of this pseudo-loop would be written $\boldsymbol{q}_\lambda == 2\pi R\Lambda_{vis} = \pi R^2\Pi$. One thus obtains the same value of the global charge $\boldsymbol{q}_\lambda$ as that obtained by considering the surface charge, which makes it possible to consider either this singularity as *a twist disclination loop* or as *a pseudo-loop of screw dislocation.*

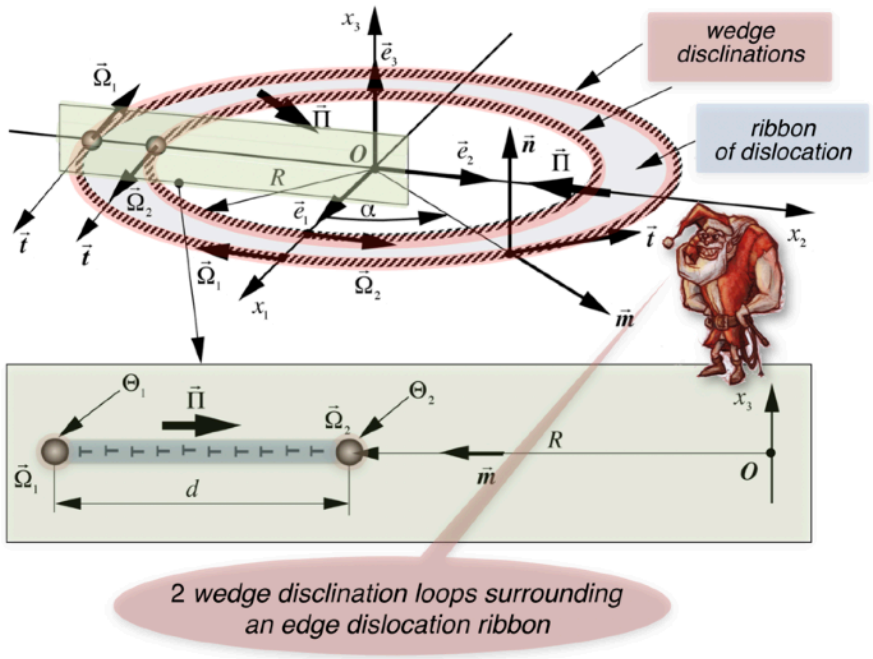

Figure 2.31 - *loop of doublet of wedge disclinations linked by a dislocation ribbon*

In figure 2.9, we have shown the macroscopic realization of *a wedge disclination loop*. But what are its main characteristics? For this, we consider a loop consisting of a doublet of wedge disclinations linked by a virtual dislocation ribbon, as shown in figure 2.31, in particular in the illustration of a section along a plane perpendicular to the plane of the loops. The linear densities of scalar charge of curvature Θ_1 and Θ_2 of the two disclinations are given by $\Theta_1 = -\vec{\Omega}_1\vec{t} = -\vec{\Pi}\vec{m}$ and $\Theta_2 = -\vec{\Omega}_2\vec{t} = -\vec{\Pi}\vec{m} = -\Theta_1$.

We deduce that the existence of these two densities Θ_1 and Θ_2 on either side of the dislocation ribbon generates a dipolar flexion field $\vec{\chi}_{dipolaire}$, located essentially in the vicinity of the two disclinations. This dipolar field is illustrated in figure 2.32 in the case of a doublet of quantized disclinations of $\pm 90°$ in a cubic structure. We can clearly see the positive and negative curvatures around the two disclinations.

It is then interesting to see that the dislocation ribbon of surface flexion charge $\vec{\Pi}$ can be reduced, by integration over the distance d separating the two disclinations, to a linear charge $\vec{\Lambda}$ of virtual edge dislocation distributed over a radius loop $R+d/2$. Thus, this loop of a doublet of disclinations can be considered similar to a loop of of edge dislocation with a linear charge $\vec{\Lambda}$ such as $\vec{\Lambda}=\vec{\Pi}d=-d\,\Theta_1\vec{\boldsymbol{m}}$.

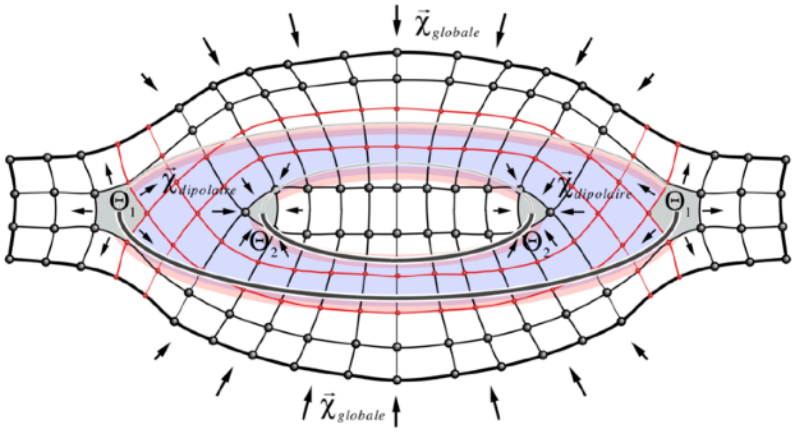

Figure 2.32 - *local dipolar field of flexion due to charges Θ_1 and Θ_2 and divergent field of flexion due to the charge $\boldsymbol{q}_\theta$ of two loops of wedge disclinations*

Such a loop of doublets of disclinations then has a global scalar charge $\boldsymbol{q}_\theta$ of curvature linked to the virtual edge dislocation ribbon which it contains, and its value is written $\boldsymbol{q}_\theta=2\pi\vec{\Lambda}\vec{\boldsymbol{m}}=2\pi\boldsymbol{B}_3=2\pi d\,\vec{\Pi}\vec{\boldsymbol{m}}=-2\pi d\Theta_1$. We can still imagine that the diameter of the internal disclination loop tends towards zero and that only the external disclination loop, of linear charge Θ_1 and radius d remains. In this case, the global charge of curvature $\boldsymbol{q}_\theta$ remains unchanged and is always given by the same relation. This global charge of curvature $\boldsymbol{q}_\theta$ is that which is due to the entire dislocation ribbon, and that which is seen at a sufficiently large distance from the loop so that it is no longer possible to distinguish this loop from a simple edge dislocation loop. The charge $\boldsymbol{q}_\theta$ is then responsible for the global flexion $\vec{\chi}_{globale}$ of the lattice at long-distance, as illustrated in figure 2.32 in the case of a doublet of quantized disclinations of $\pm 90°$ in a cubic structure.

Clusters of dislocations, disclinations and dispirations

Since *the dislocation, diclination and dispiration strings* containing non-zero densities of tensor charges can be closed on themselves in the form of loops, it is quite possible to imagine the existence of small very localized clusters of such loops within a solid medium. Such clusters are in principle entirely characterized by their tensor density $\vec{\lambda}_i$ of dislocation charges, which take a non-zero value within the strings, in the field of the cluster.

As the cluster is composed exclusively of loops closing in on themselves, there are no vectors $\vec{\boldsymbol{B}}$ and / or $\vec{\Omega}$ with non-zero value on any contour surrounding the cluster without crossing it, which implies that there is no discontinuities of the virtual displacement field $\vec{u}^{(\delta)}$ nor

discontinuities of the local rotation field $\vec{\omega}^{(\delta)}$ in the part of the solid surrounding the cluster, and that, consequently, the solid remains perfect outside the cluster.

However, the presence of the cluster within the solid must certainly imply a field of elastic and anelastic distortions of the perfect solid surrounding the cluster and up to a certain distance from it, just like the presence of a density ρ of localized electric charges implies an electric displacement field $\vec{D}$ remote from these electric charges.

To find this field, it is necessary to bring into play here the fact that there is, apart from the conservation equation $\mathrm{div}\,\vec{\lambda}_i \equiv 0$ of the tensorial charge, no restriction on the scalar densities λ and θ of charges of rotatio and flexion. Consequently, it is entirely possible that, depending on the nature of the charges making up the cluster, it may have non-zero global scalar charges of rotation $\boldsymbol{Q}_\lambda$ and curvature $\boldsymbol{Q}_\theta$, defined by the sums on all the closed loops of the global charges $\boldsymbol{q}_{\lambda(i)}$ and $\boldsymbol{q}_{\theta(i)}$ as defined above for each individual loop in the previous section. One can imagine, for example, that the charge of curvature of a cluster could be due to prismatic dislocation loops, of lacunar or interstitial nature (figure 2.29) and / or wedge disclinations loops (figure 2.31), and that the rotation charge could be due to twist disclination loop (figure 2.30).

These considerations then make it possible to find the fields of elastic and anelastic distortions implied at a great distance by the presence of a localized cluster of charges. The presence of a non-zero global scalar charge $\boldsymbol{Q}_\lambda$ of rotation in a localized cluster of charges behaves as the source of a divergent field of rotation $\vec{\omega}$ within the perfect solid surrounding the cluster of charges (figure 2.33). The field of rotation then presents *a topological singularity* at the place where the cluster of charge $\boldsymbol{Q}_\lambda$ is located, and its norm $|\vec{\omega}|$ presents a decrease in $1/R^2$ at long distance from the cluster.

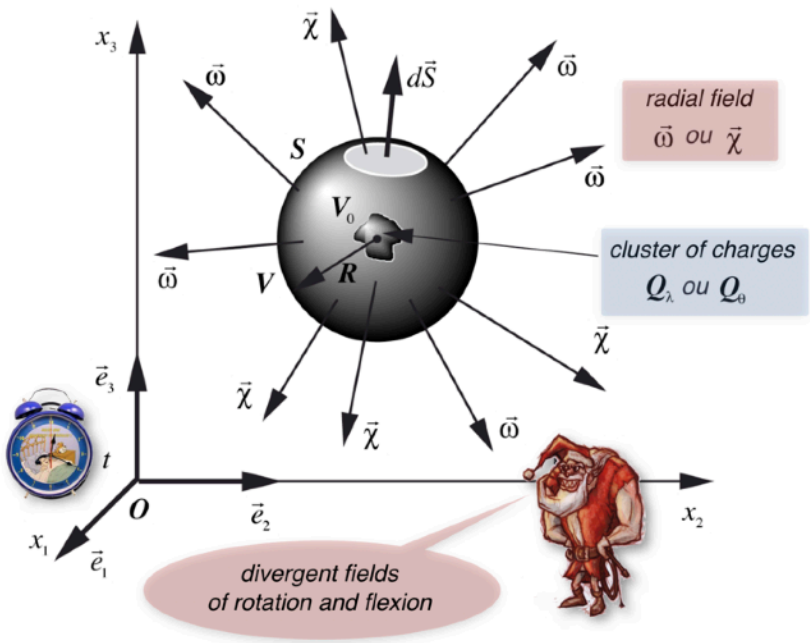

Figure 2.33 - *Divergent fields of rotation and flexion in the vicinity of a cluster of charges*

Everything in fact happens exactly as in electromagnetism, where a localized density ρ of electric charges, leading to a localized macroscopic electric charge $\boldsymbol{Q}$, behaves like a singularity responsible for a field of electric displacement $\vec{D}$ diverging in the surrounding space.

A macroscopic scalar load $\boldsymbol{Q}_\theta$ of nonzero curvature behaves as *the source of a divergent field* $\vec{\chi}$ *of flexion* within the perfect solid surrounding the cluster of charges (figure 2.33). The bending field then presents *a topological singularity* at the place where the cluster of charges $\boldsymbol{Q}_\theta$ is located, and its norm $\boldsymbol{Q}_\theta$ also presents a decrease $1/R^2$ at long distance from the cluster. In other words, in the vicinity of a global localized load $\boldsymbol{Q}_\theta$ of curvature, the solid presents curvatures by bending of spherical symmetry around the singularity.

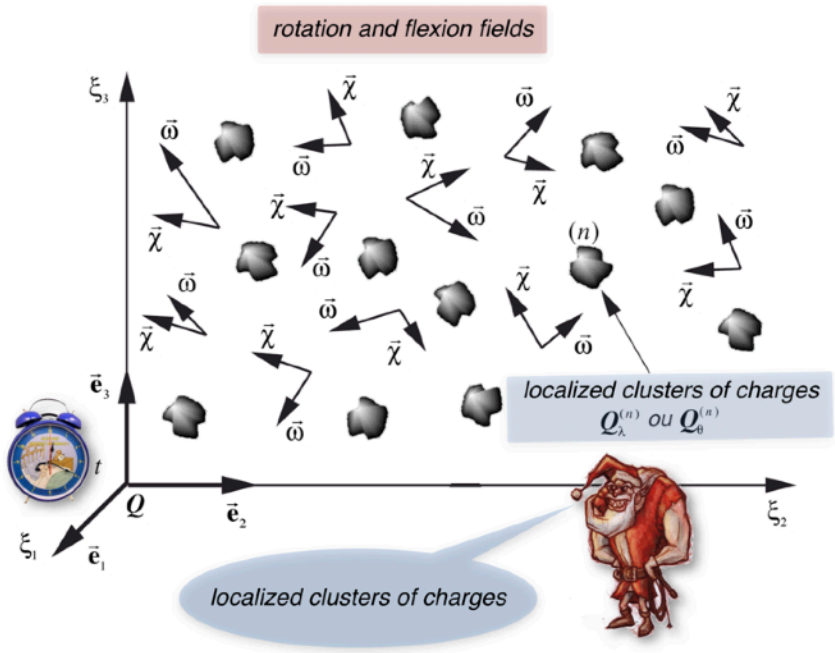

Figure 2.34 - *Description of a solid containing localized clusters of charges*

Let be *a hypothetical solid* in which the charges are confined in localized clusters, as illustrated for example in figure 2.34, and therefore in which *there are no dislocation and disclination strings propagating over great distances* compared to the scale at which solid is studied. It is clear that, depending on the complexity of the internal structure of these clusters, in other words the complexity of the entanglement of the loops making up these clusters, the description of the fields of distortion and contortion within the clusters themselves can be very complex. But if these clusters have stable internal structures and they can move individually within the solid, but without interacting enough between them to modify their internal structure, it is possible to greatly simplify the description of the distortion fields prevailing in this solid.

In this case indeed, and insofar one is essentially interested in describing the elastic and anelastic distortion and contortion fields in the domains of the perfect solid, that is to say at a certain distance from the outside the clusters of charges, the problem can be solved much more simply by considering only the scalar charge densities λ and θ inside the clusters, which can result at great distance by the existence of two macroscopic scalar charges $\boldsymbol{Q}_{\lambda(n)}$ and $\boldsymbol{Q}_{\theta(n)}$ for each cluster number (n).

In fact, the knowledge of the distribution of charge density λ and θ inside a cluster makes it possible to find purely topological conditions, and consequently independent of the elastic properties of the solid considered, which are imposed on the fields of rotation $\vec{\omega}$ and flexion $\vec{\chi}$ reigning in the perfect solid outside the cluster. These conditions are simply expressed by the scalar equations of geometro-compatibility $\lambda = \mathrm{div}\vec{\omega}$ and $\theta = \mathrm{div}\vec{\chi}$. Depending on the inhomogeneity of the internal distribution of charge densities λ and θ in the cluster, it can then appear *dipolar or multipolar fields* $\vec{\omega}$ *and* $\vec{\chi}$ *at short and medium distance from each cluster.*

On the other hand, *at large distances from clusters of charges*, it is essentially the presence of macroscopic scalar charges $\boldsymbol{Q}_{\lambda(n)}$ and $\boldsymbol{Q}_{\theta(n)}$ which are different from zero which will be responsible for the appearance of monopolar radial fields of rotation $\vec{\omega}$ and flexion $\vec{\chi}$, as already illustrated in figure 2.33.

Thus, in this particular case of charges located in clusters, it is *the two invariant vector fields*, namely the fields of rotation $\vec{\omega}$ and flexion $\vec{\chi}$, which are affected at a certain distance from the clusters of charges. And it is quite remarkable that each of these clusters can be individually and completely characterized, as for its long-range effects on the fields of distortion and contortion, by its only two macroscopic scalar charges $\boldsymbol{Q}_{\lambda(n)}$ and $\boldsymbol{Q}_{\theta(n)}$, even so these clusters can have very complex core structures, of tensorial nature, therefore very strongly dependent on their spatial orientation in the local frame of reference.

In the analogy previously developed with electromagnetism, the field of rotation $\vec{\omega}$ is the analog of electric displacement $\vec{D}$, and the macroscopic charge of rotation $\boldsymbol{Q}_{\lambda(n)}$ is the analog of the macroscopic electric charge $\boldsymbol{Q}$ of a corpuscle in electromagnetism. But is there also a similar analogy for the flexion field $\vec{\chi}$ and the overall charge $\boldsymbol{Q}_{\theta(n)}$ of curvature?
A partially positive answer can be given here. Indeed, the presence of a cluster of macroscopic flexion charge $\boldsymbol{Q}_{\theta(n)}$ is responsible for a non-zero and divergent vector flexion field $\vec{\chi}$ in its vicinity, therefore for *a spatial curvature of the solid lattice* surrounding this cluster, which results in the appearance of non-zero shear strain fields and volume expansion fields. Thus, the presence of a cluster of charges such as $\boldsymbol{Q}_{\theta(n)} \neq 0$ implies, vis-à-vis the solid lattice, a result presenting a certain analogy with that stipulated by the theory of general gravitation of Einstein vis-à-vis the space-time in the presence of matter, namely that a cluster of matter located in a place of space is directly responsible for a curvature of the neighboring space-time. We will come back to this analogy in detail later.

Flow of dislocation charges

The macroscopic interpretation of the density tensors $\vec{\lambda}_i$ of dislocation charges as well as the conservation equation $\mathrm{div}\vec{\lambda}_i \equiv 0$ which these tensors satisfy have revealed the notion of strings and loops of dislocation, disclination and dispiration. It has also been shown that at large distances from clusters of plastic charges, it is essentially the two invariant vector fields, namely the fields of rotation $\vec{\omega}$ and curvature $\vec{\chi}$, which are affected by the scalar components λ and θ of charges. It now remains to make the link between these quantities and the charge flows $\vec{J}_i$ and $\vec{J}$ introduced into the geometro-kinetic equations of figure 2.5.

Let us therefore consider a tube filled with a density $\vec{\lambda}_i$ of dislocation charges, which moves at *relative velocity* $\vec{\boldsymbol{v}}$ *with respect to the lattice*, where the velocity is measured perpendicular to the direction of the tube. We can show that the relation existing between the tensor density of

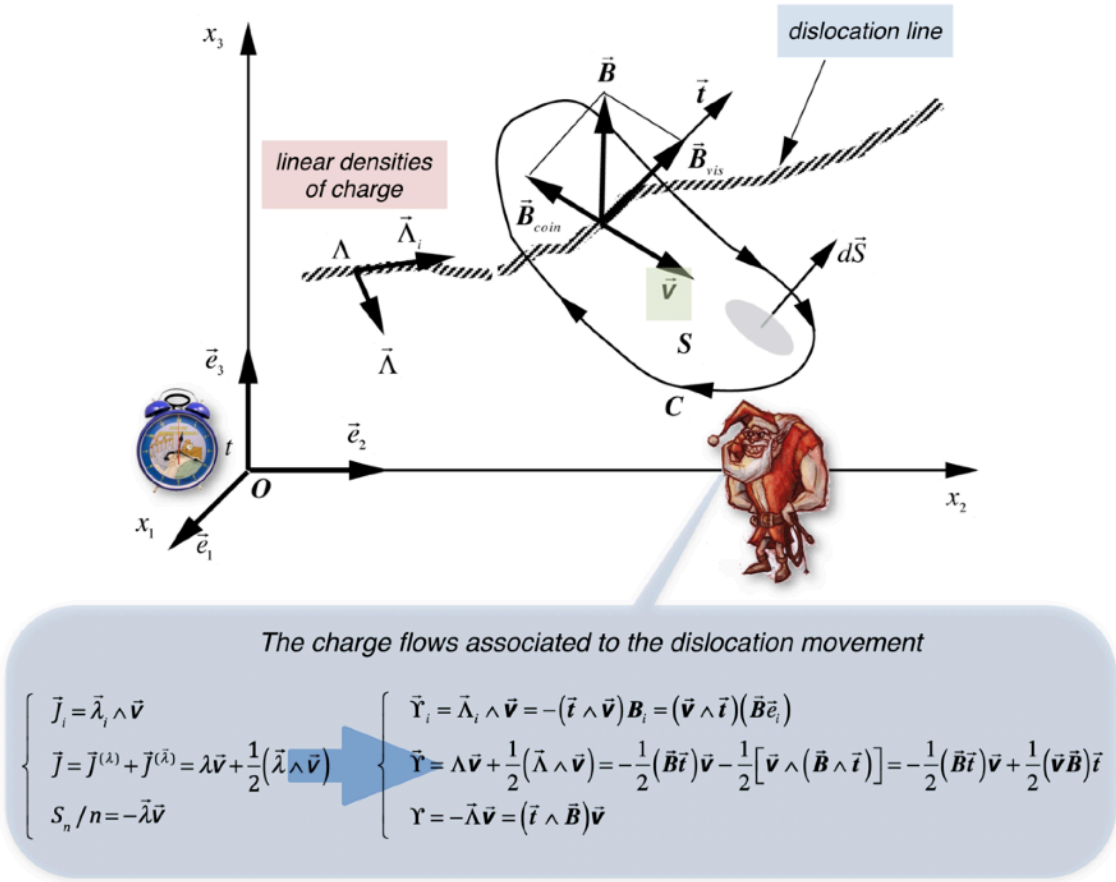

Figure 2.35 - *The charge flows associated to a dislocation line moving at velocity* $\vec{\boldsymbol{v}}$ *in the frame* $\boldsymbol{Ox_1x_2x_3}$

charge $\vec{\lambda}_i$ in motion at speed $\vec{\boldsymbol{v}}$ with respect to the lattice and *the tensorial flux* $\vec{J}_i$ *of charges* which is associated with this movement is then written $\vec{J}_i = \vec{\lambda}_i \wedge \vec{\boldsymbol{v}}$, from which we also deduce *the vector flux of charges* $\vec{J} = \vec{J}^{(\lambda)} + \vec{J}^{(\vec{\lambda})} = \lambda\vec{\boldsymbol{v}} + \left(\vec{\lambda} \wedge \vec{\boldsymbol{v}}\right)/2$ and the scalar source of sites $S_n / n = -\vec{\lambda}\vec{\boldsymbol{v}}$.

We can apply this relation to the case of dislocation lines. We consider a dislocation line like the one shown in figure 2.35, which moves to the velocity $\vec{\boldsymbol{v}}$ relative to the lattice. It is clear that, in the case of a line, the velocity $\vec{\boldsymbol{v}}$ can only be perpendicular at all points to the direction $\vec{\boldsymbol{t}}$ of the line. In the case of a line, one can integrate (summate) the vectorial flow $\vec{J}_i$ of charges on the surface of the contour $\boldsymbol{C}$ surrounding the dislocation line and mobile with it. The integrations on the surface of the contour of the charge fluxes $\vec{J}_i$ and $\vec{J}$ will give *the linear fluxes associated with the mobile dislocation*, that is to say the total fluxes per length unit of dislocation, which will be represented by the symbols $\vec{\Upsilon}_i$ and $\vec{\Upsilon}$. As the flows $\vec{J}_i$ and $\vec{J}_i$ have as dimension the inverse of a time (1/s), the linear flows $\vec{\Upsilon}_i$ and $\vec{\Upsilon}$ will have as dimension a surface per unit of time (m²/s). As for the source S_n / n of network sites, its integral will also represent a surface per unit of time (m²/s), and we will write it Υ. It then comes the relations reported in figure 2.35, which connect *the linear fluxes* $\vec{\Upsilon}_i$ and $\vec{\Upsilon}$, as well as *the linear source* Υ *of sites* to the *linear densities of charge* $\vec{\Lambda}_i$, $\vec{\Lambda}$ and Λ *of*

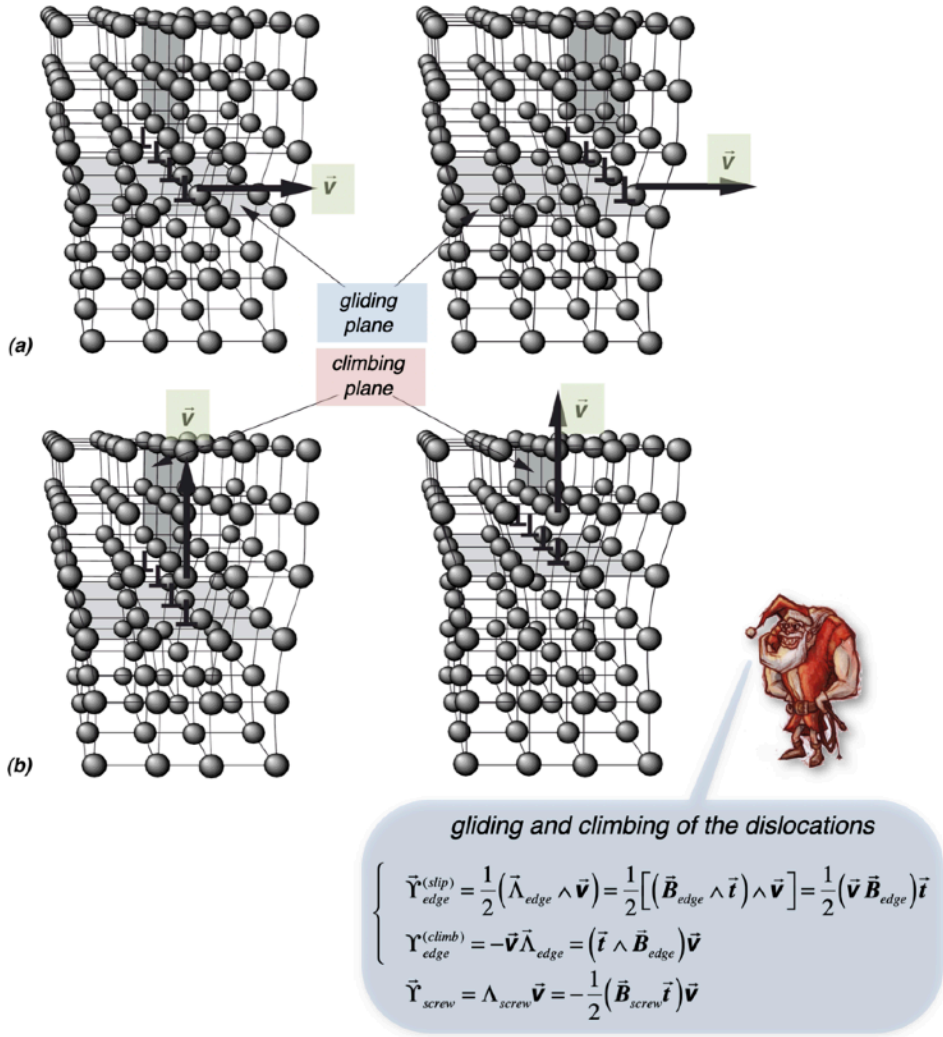

Figure 2.36 - *The movements of gliding* ***(a)*** *and of climbing* ***(b)*** *of an edge dislocation*

dislocations. We also deduce the relations directly linking the linear fluxes $\vec{\Upsilon}_i$, $\vec{\Upsilon}$ *and* Υ to the Bürgers vector $\vec{\boldsymbol{B}}$ of the dislocation.

If the dislocation has only one screw component, the flux $\vec{\Upsilon}_{screw}$ will be given by the relation reported in figure 2.36. This relation shows that, as the velocity $\vec{\boldsymbol{v}}$ is always perpendicular to the direction $\vec{\boldsymbol{t}}$ of the line, the purely screw dislocations can move in all the directions perpendicular to the direction $\vec{\boldsymbol{t}}$. In this case we speak of a *gliding movement of the screw dislocations*, and the planes on which the screw dislocation moves are called *gliding planes*.

In the case of a purely edge dislocation, two possible types of movement appear, leading to linear flows $\vec{\Upsilon}_{edge}^{(gliding)}$ and $\Upsilon_{edge}^{(climb)}$ whose mathematical expressions are shown in figure 2.36:
- the movement for which $\vec{\boldsymbol{v}}$ is perpendicular to $\vec{\Lambda}$, and which is responsible for a vector charge flow $\vec{\Upsilon}_{edge}^{(gliding)}$. This movement is shown in figure 2.36a. It corresponds to a conservative movement of *gliding* of the edge dislocation on its *gliding plane*, defined as the plane perpendicular to $\vec{\Lambda}$, therefore the plane which contains at the same time the Burgers vector $\vec{\boldsymbol{B}}_{edge}$, the direction $\vec{\boldsymbol{t}}$ of the line and the velocity vector $\vec{\boldsymbol{v}}$.
- the movement for which $\vec{\boldsymbol{v}}$ is parallel to $\vec{\Lambda}$, and which is responsible for a scalar charge flow $\Upsilon_{edge}^{(climb)}$. This movement is shown in figure 2.36b. It corresponds to a non-conservative

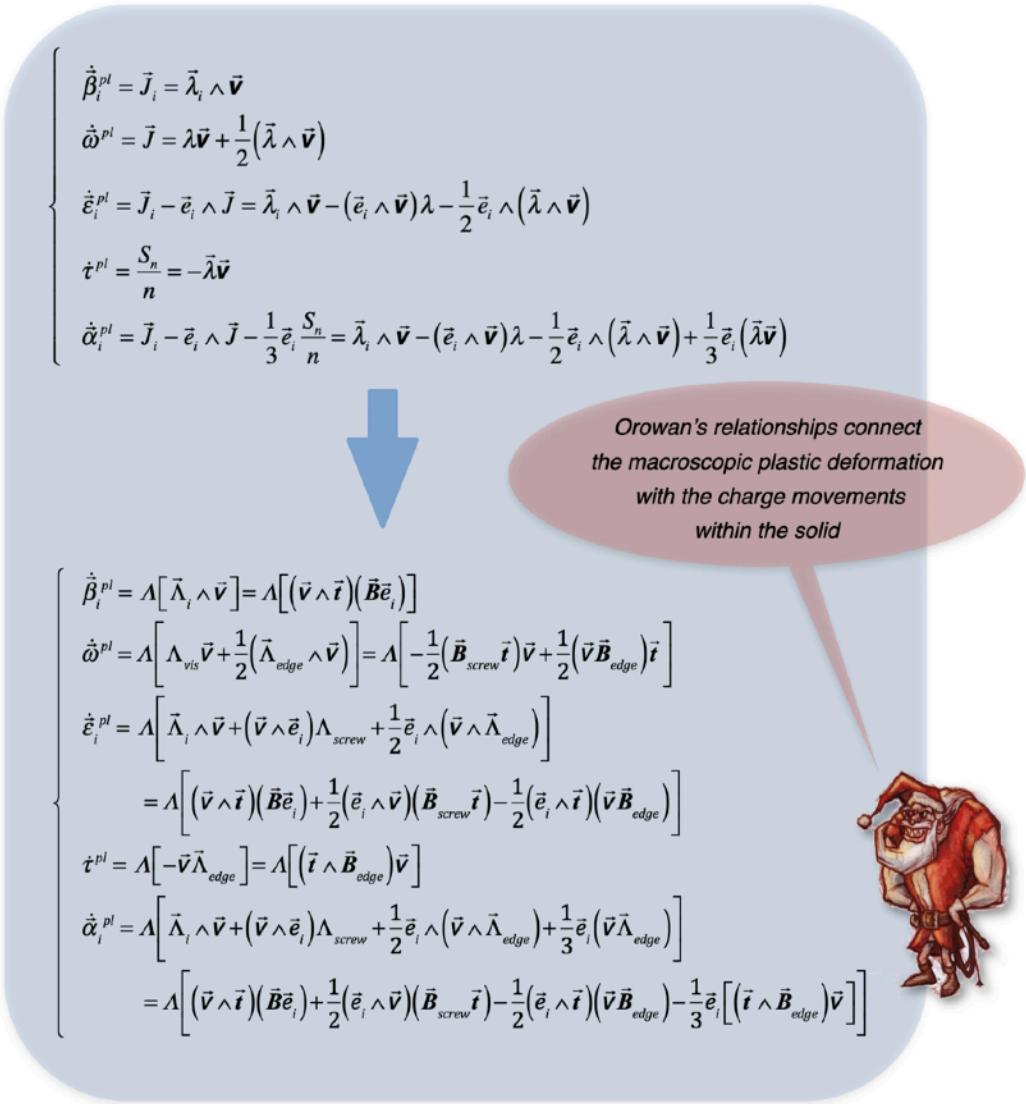

Figure 2.37 - *The Orowan's relation which connect the plastic distortions to the movements of the charges*

movement of *climb* of the edge dislocation perpendicular to its gliding plane. Dislocation *«is climbing»* in the lattice, creating or destroying a lattice plan. This movement is therefore non-conservative in the sense that it destroys or builds the lattice, and it is this movement which is responsible for the existence of a source S_n of lattice sites in the geometro-kinetic equation of the volume expansion reported in figure 2.5, which is written as $S_n = -n\vec{\boldsymbol{v}}\vec{\Lambda}_{coin} = n\left(\vec{\boldsymbol{t}} \wedge \vec{\boldsymbol{B}}_{coin}\right)\vec{\boldsymbol{v}}$.

It is the movement of dislocation charges that is responsible for the macroscopic plastic deformation of a solid. From the knowledge of the dislocation charge flows $\vec{J}_i$, it is then possible to go back to *the macroscopic plastic distortions* $\vec{\beta}_i^{\,pl}$ of the solid thanks to the famous *Orowan relations*. The total derivatives along the medium trajectory of the macroscopic plastic distortions $\dot{\vec{\beta}}_i^{\,pl}$, $\dot{\vec{\varepsilon}}_i^{\,pl}$, $\dot{\vec{\alpha}}_i^{\,pl}$, $\dot{\vec{\omega}}^{pl}$ and $\dot{\tau}^{pl}$ of the charged solid are reported in figure 2.37, as a function of the volume densities of charges $\vec{\lambda}_i$, $\vec{\lambda}$ and λ, as a function of the linear densities of charges $\vec{\Upsilon}_i$, $\vec{\Upsilon}$ and Υ associated with the movement of dislocation lines, and finally as a function of the Burgers vectors of dislocations in place of the linear densities of charge of the dislocation lines.

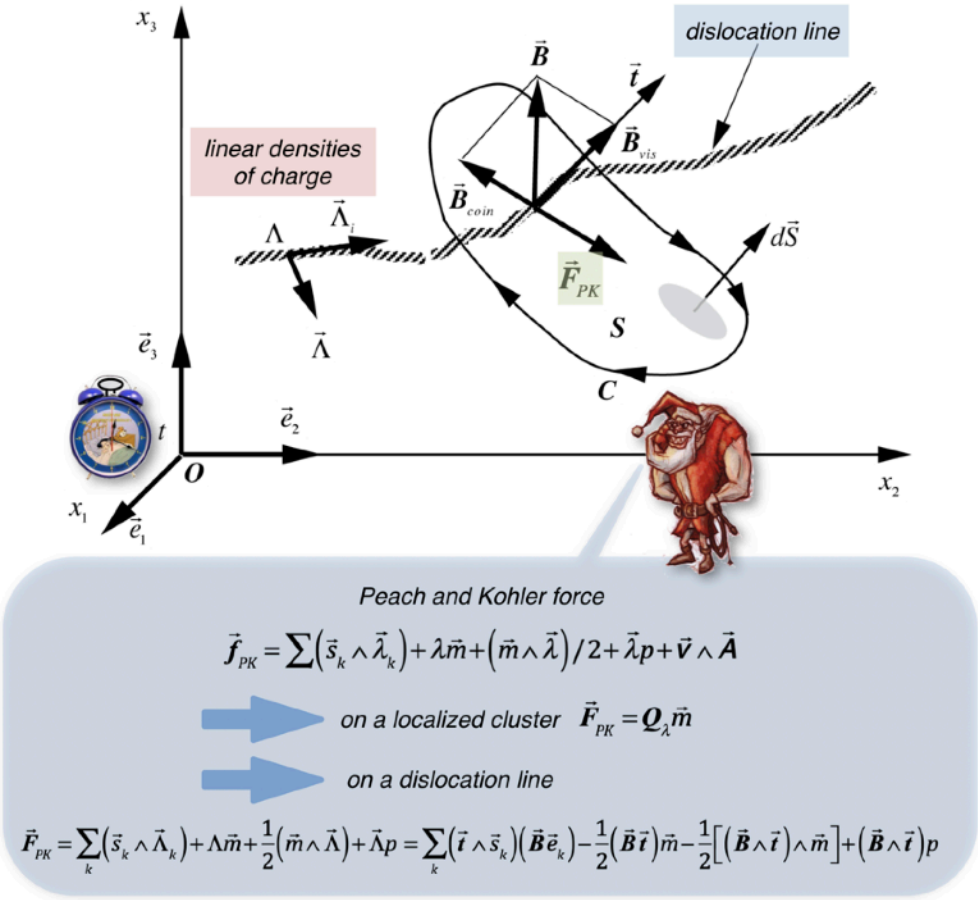

Figure 2.38 - *The Peach et Koehler force* $\vec{F}_{PK}$ *acting on the topological singularities*

Force of Peach and Kohler acting on a line of dislocation

By establishing the energy balance equation of a solid containing dislocations, a power term $P_{ch} = \vec{s}_k \vec{J}_k + \vec{m}\vec{J} - pS_n / n$ appears which is nothing other than the power supplied to the charges by the stress fields $\vec{s}_k, \vec{m}, p$ appearing within the deformable solid.In this term of power, it is possible to replace the fluxes $\vec{J}_k$, $\vec{J}$ and S_n / n by their expressions according to the velocity $\vec{v}$ of the charges, taken from figure 2.35. There comes an expression of P_{ch} containing this time the charge densities $\vec{\lambda}_k$, $\vec{\lambda}$ and λ. The power P_{ch} supplied to the charges is therefore the product $P_{ch} = \vec{f}_{PK}\vec{v}$ of a velocity by a term which can only be a force $\vec{f}_{PK}$ acting on the charge densities $\vec{\lambda}_k, \vec{\lambda}, \lambda$ per volume unit. The expression obtained for this force is shown in figure 2.38.

This force which depends on the stress tensors $\vec{s}_k$, $\vec{m}$ and / or p is generally called *the Peach and Koehler force*. As the dimension of $\vec{\lambda}_k, \vec{\lambda}, \lambda$ is the inverse of a length (1/m) and since the dimension of the moment vector is a moment per unit of volume, namely (Nm/m^3), the force has for dimension a force by volume unit (N/m^3). The last term containing *a vector* $\vec{A}$ is added here because it is *a force term which would not produce work*, and therefore would not appear in the expression of power P_{ch}. We will see later that this term actually corresponds to a relativistic force analogous to *the Lorentz force* in electromagnetism.

The force of Peach and Koehler can also be written in the case of a dislocation, by

integrating the relation giving $\vec{f}_{PK}$ on the surface of a section of the string. It then comes, neglecting for the moment the term containing the vector $\vec{A}$, the expressions of the Peach and Koehler force acting on a dislocation line which are shown in figure 2.38, expressed respectively from the linear charge densities $\vec{\Lambda}_i$, $\vec{\Lambda}$ and Λ of the dislocations, and from the Bürgers vector $\vec{B}$ of the dislocation.

The dimension of the force $\vec{F}_{PK}$ acting on the dislocation is a force per unit of length (N/m). This is actually *the force per unit length of the line* in the presence of the stress fields $\vec{s}_k, \vec{m}, p$. The writing of the Peach and Koehler force $\vec{F}_{PK}$ using the stress tensors $p, \vec{m}, \vec{s}_k$ is very interesting, because it allows to make a much clearer representation than with the notation usually used in the literature which exclusively uses the symmetrical stress tensor $\vec{\sigma}_k$. Indeed, suppose a solid in which the volume expansion is zero, and therefore which would have a negligible pressure p. In this case, we know that we can replace the shear strain tensor $\vec{\alpha}_k$ with the rotation vector $\vec{\omega}$, so that the force becomes a gliding force which can be written $\vec{F}_{PK} = \Lambda\vec{m} + \left(\vec{m} \wedge \vec{\Lambda}\right)/2$, in which the term $\Lambda\vec{m}$ is the force acting on the screw component of the dislocation and the term $\left(\vec{m} \wedge \vec{\Lambda}\right)/2$ is the force acting on the edge component of the dislocation. As the component m_k of the moment of rotation is associated with the components σ_{ij} and σ_{ji} of the shear strain tensor, one can immediately make a very clear representation of the forces acting on a dislocation. The same goes for the pressure force $\vec{\Lambda}p$, which acts only on the edge component $\vec{\Lambda}$ of the dislocations and which corresponds, given its direction (figure 2.36), to *a climbing force on the dislocations.*

In the case of a localized charge Q_λ of rotation, one obtains the force of Peach and Koehler by integrating the force on all the volume of the localized charge. The result is shown in figure 2.38. In this case, the dimension of $\vec{F}_{PK} = Q_\lambda \vec{m}$ is that of a pure force, expressed in (N), and which is the analog of the electric force $\vec{F}_{électrique} = q\vec{E}$ acting on a localized electric charge in electromagnetism.

Potentialities of the Eulerian representation of charged lattices

The tensor density $\vec{\lambda}_i$ and the tensor flux $\vec{J}_i$ of dislocation charges defined in this chapter make it possible to find the set of fundamental and phenomenological equations of spatio-temporal evolution which must be satisfied by an anelastic and self-diffusing solid lattice containing dislocation charges. This development is done with many details in my first book. We will only describe here very briefly two important aspects which can be treated in the context of the Eulerian representation of solid media containing plastic charges.

It is possible to combine all the results described so far to obtain the complete space-time evolution equations of a solid self-diffusing lattice, presenting phenomenological behaviors of elasticity and anelasticity, and containing dislocation charge densities and flows. As figure 2.39 shows, this system of equations is quite complex, especially at the level of the large number of phenomenological state equations and phenomenological dissipation equations necessary for a complete description of all possible phenomena in such an environment, and which we will not tackle in this book.

The concepts of densities and flow of dislocation charges make it possible to describe the phenomena of plasticity and anelasticity at the microscopic level of the discrete solid lattice, by introducing into it an evolutionary microstructure of plastic charges which should make it

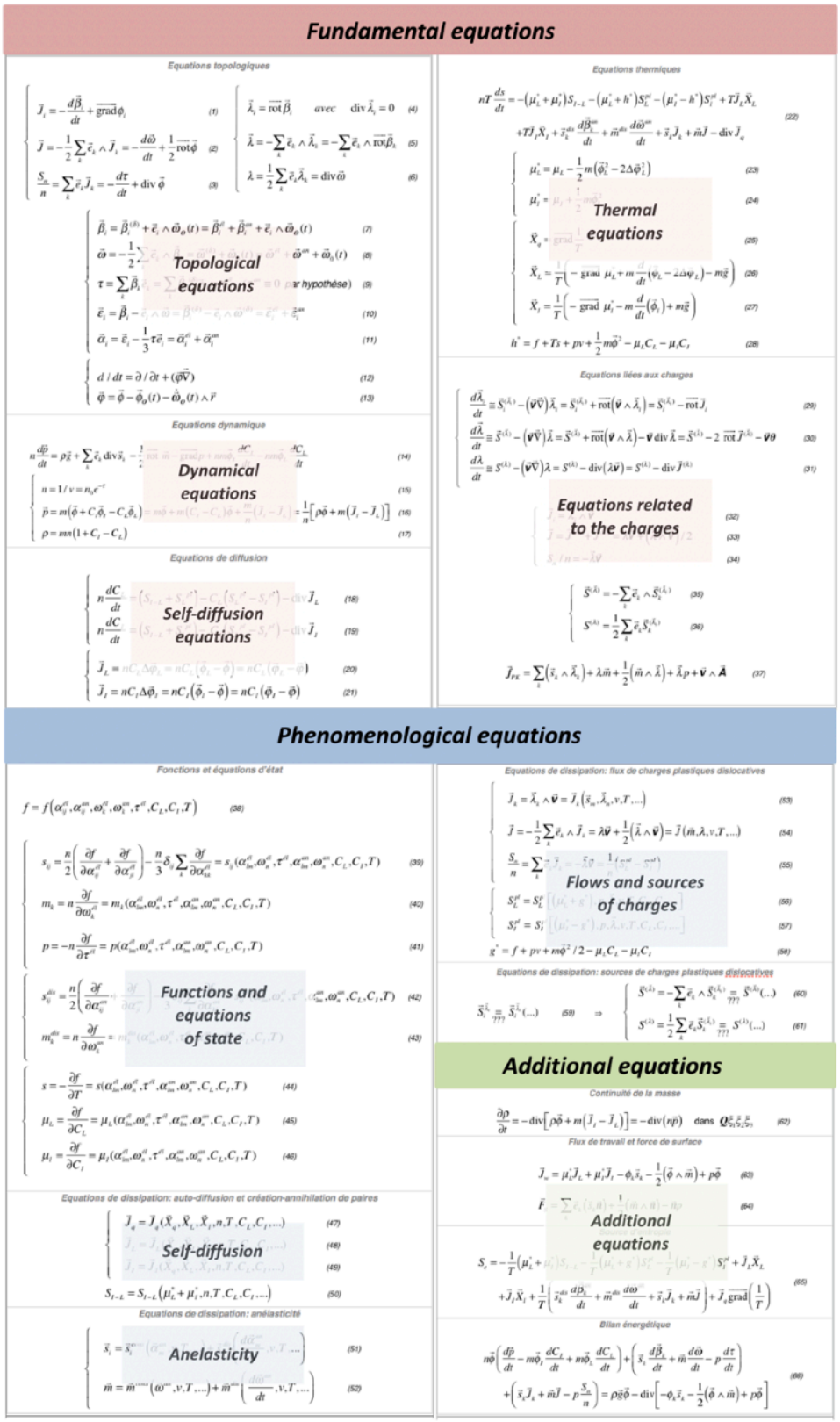

Figure 2.39 - *Synoptic representation of fundamental and phenomenological equations necessary for the description of the spatio-temporal evolution of a solid medium presentig elasticity, anelasticity and self-diffusion, and containing mobile plastic charges.*

possible to translate the non-Markovian behaviors of plasticity. In addition, the approach using plastic charges at the microscopic level of the discrete solid lattice also makes it possible in principle to find exact local expressions for the dissipative equations linked to plastic charges.

By introducing the simplest solid which it is possible to consider, namely the isotropic perfect solid, one can obtain *the Newton's equation* of this solid. We can then show that this solid is perfectly described by *equations similar to Maxwell's equations* when *the volume expansion is homogeneous within the solid*.

One can also calculate the fields of distortions, the energies and the interactions of the dislocations in this perfect solid. In the case of stationary dislocations in the solid lattice, *the static distortions of the lattice* induced by them store elastic energy within the lattice. This stored energy can then be considered as *the rest energy of the dislocations*. In the case where the dislocations are mobile in the lattice, the displacements of the lattice induced by the movement of the dislocations are associated with kinetic energy. At low speed, this kinetic energy is directly linked to the rest energy of these dislocations via relations similar to *the famous expression of Einstein* $E_0 = M_0 c^2$, which makes it possible to introduce in a completely classic way the concept of *mass of inertia of the dislocations*.

From the distortion fields induced by the dislocations and from the Peach and Koehler force, we can also describe the interactions that can occur between dislocations.

Finally, we can also introduce *the string model,* which will allow us to deal with the dynamics of a dislocation that moves in the lattice while being deformed. The string model has proven to be extremely useful and efficient in dealing with plasticity and anelasticity problems due to the movement of dislocations and occurring in common solids, such as metals for example. But it is not within the purview of this book to deal in detail with the problem of these phenomena, which can be addressed in many books dealing with this particular subject. However, to arouse the interest of the reader, we have plotted the equation of the string of a dislocation in figure 2.40a, and, by way of example, two typical applications:

- *the thermally activated interaction of a dislocation with a field of punctual obstacles:* to introduce this type of interactions into the string model, it is necessary to know the spatial distribution of obstacles in the solid, as well as the internal stress fields generated by them. These stress fields due to obstacles can be expressed and visualized at the level of the gliding plane of the dislocation, as illustrated in figure 2.40b, where it appears many Peach and Koehler forces $\sum \boldsymbol{f}_n\left(x_1, u(x_1,t)\right)$ combining to act on the dislocation. But the string equation in figure 2.40b in the presence of interactions with obstacles is a purely mechanical equation, which cannot take into account temperature effects, such as the migration of obstacles by diffusion or the crossing of obstacles by thermal activation. Introducing the effects of temperature into the string equation is theoretically possible by developing *a "Brownian" image* of the dislocation, that is, by introducing a term of local thermal fluctuations $\boldsymbol{F}_{fluctuation}\left(x_1, u(x_1,t), t\right)$ into the string equation, as illustrated in figure 2.40c, modeled on the term of thermal fluctuations in the model of *the Langevin equation*. It is clear that such an approach to the dynamics of dislocation quickly proves to be very complex.

In general, these problems of dislocation interactions with obstacles are approached in a much more pragmatic way, by developing, on the basis of the string model, simplified models judiciously adapted to the problem to be treated. To deepen this subject, one will find examples

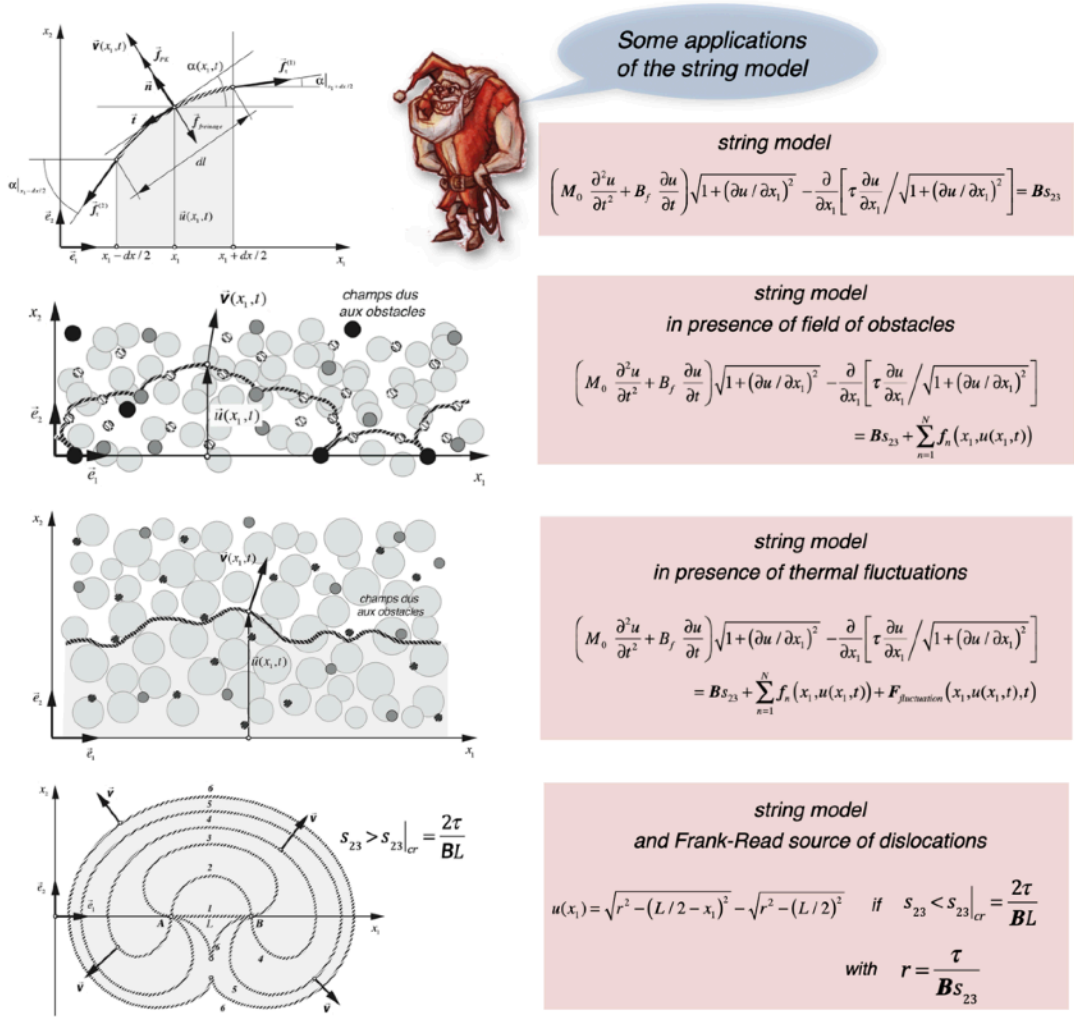

Figure 2.40 - *The string model and some of its applications*

of mechanisms of interaction of dislocations with obstacles, illustrated by experimental results and theoretical models, in many books dealing with dislocations, or in a more summarized way in review articles such as *"Dislocation-point defect interactions"*[11] and *"dislocation-lattice interactions»*[12]*.*

- *the source of Frank-Read dislocations:* we now suppose a dislocation segment of length L anchored on its gliding plane at two points ***A*** and ***B*** located on the axis Ox_1 in $x_1 = 0$ and $x_1 = L$, as illustrated in figure 2.40d. Such anchoring points can be due to the existence of strong and localized interactions of the dislocation with obstacles (other dislocations, precipitates, etc.). Using the string equation in the static case, it is fairly easy to show that the deformation of the dislocation segment under the effect of a static stress is a portion of a circle whose radius depends on the stress s_{23} applied to the solid. In fact, the radius of curvature of

---

[11] *G. Gremaud, chap.3.3, dans «Mechanical spectroscopy», Trans Tech Publications, Zürich, 2001, p.178-246*

[12] *W. Benoit, chap. 3.2, dans «Mechanical spectroscopy», Trans Tech Publications, Zürich, 2001, p. 158-177*

the segment is inversely proportional to the static shear stress s_{23}, which means that the latter decreases as s_{23} increases. However, it is clear that there is a minimum limit for the radius of curvature, which intervenes for a critical stress $s_{23}\big|_{cr}$ such that the radius of curvature becomes equal to $L/2$. For any value s_{23} greater than $s_{23}\big|_{cr}$, there can be no static solution for the deformation of the string segment. There then appears a complex dynamic solution to the equation of the string, which in fact corresponds to *a Frank-Read source mechanism*.

The initial straight segment shown by *(1)* in Figure 2.40d curves between the two anchor points until it forms a semicircle *(2)*. Then it continues to extend beyond the anchoring points, steps *(3), (4)* and *(5)*, until the strand of the segment leaving from ***A*** joins the strand of segment leaving from ***B*** *(6)* . At this point, as the two strands have the same Burgers vector, they bind together by forming on the one hand a new segment *(1)* growing between the anchoring points ***A*** and ***B*** , and on the other hand a closed loop *(6)* which will not stop growing. This mechanism therefore constitutes a phenomenon of uninterrupted source of dislocation loops. It is essentially this phenomenon, which is very well observed by electron microscopy, which explains why it is possible to carry out significant plastic deformations of certain solids such as metals. And it is indeed this type of phenomenon which can be responsible for the existence of a non-zero source of dislocation charges in the equation of continuity of the density of dislocation charges in Figure 2.5, which induces a non-commutativity of the operator of material derivative with the operators of space.